MARTIN MARIETTA ENERGY SYSTEMS LIBRARIES

3 4456 0355939 8

ornl

ORNL-6629/P2

OAK RIDGE
NATIONAL
LABORATORY

MARTIN MARIETTA

Evaluation of Advanced Austenitic Alloys Relative to Alloy Design Criteria for Steam Service—Part 2—20 to 30% Chromium Alloys

R. W. Swindeman
P. J. Maziasz

OAK RIDGE NATIONAL LABORATORY
CENTRAL RESEARCH LIBRARY
CIRCULATION SECTION
4500N ROOM 175
LIBRARY LOAN COPY
DO NOT TRANSFER TO ANOTHER PERSON
If you wish someone else to see this report, send in name with report and the library will arrange a loan.
UCN-7969 (3 9-77)

Fossil
Energy
Program

MANAGED BY
MARTIN MARIETTA ENERGY SYSTEMS, INC.
FOR THE UNITED STATES
DEPARTMENT OF ENERGY

This report has been reproduced directly from the best available copy.

Available to DOE and DOE contractors from the Office of Scientific and Technical Information, P.O. Box 62, Oak Ridge, TN 37831; prices available from (615) 576-8401, FTS 626-8401.

Available to the public from the National Technical Information Service, U.S. Department of Commerce, 5285 Port Royal Rd., Springfield, VA 22161.

This report was prepared as an account of work sponsored by an agency of the United States Government. Neither the United States Government nor any agency thereof, nor any of their employees, makes any warranty, express or implied, or assumes any legal liability or responsibility for the accuracy, completeness, or usefulness of any information, apparatus, product, or process disclosed, or represents that its use would not infringe privately owned rights. Reference herein to any specific commercial product, process, or service by trade name, trademark, manufacturer, or otherwise, does not necessarily constitute or imply its endorsement, recommendation, or favoring by the United States Government or any agency thereof. The views and opinions of authors expressed herein do not necessarily state or reflect those of the United States Government or any agency thereof.

ORNL-6629/P2

Metals and Ceramics Division

EVALUATION OF ADVANCED AUSTENITIC ALLOYS RELATIVE TO ALLOY DESIGN CRITERIA FOR STEAM SERVICE - PART 2 - 20 TO 30% CHROMIUM ALLOYS

R. W. Swindeman and P. J. Maziasz

Date Published: June 1991

Prepared for the
U.S. Department of Energy,
Office of Fossil Energy,
Advanced Research and Technology
Development Materials Program
AA 15 10 10 0

Notice: This document contains information of a preliminary nature. It is subject to revision or correction and therefore does not represent a final report.

Prepared by the
OAK RIDGE NATIONAL LABORATORY
Oak Ridge, Tennessee 37831-6285
managed by
MARTIN MARIETTA ENERGY SYSTEMS, INC.
for the
U.S. DEPARTMENT OF ENERGY
under Contract DE-AC05-84OR21400

MARTIN MARIETTA ENERGY SYSTEMS LIBRARIES

3 4456 0355939 8

CONTENTS

LIST OF TABLES v

LIST OF FIGURES vii

ABSTRACT 1

1. INTRODUCTION 1

2. MATERIALS 2

3. METALLURGICAL STABILITY 4

4. FABRICATION AND JOINING 14

5. MECHANICAL PROPERTIES 26

6. TENSILE PROPERTIES 29

7. STRESS-RUPTURE 29

8. FIRESIDE CORROSION 44

9. STEAMSIDE CORROSION 45

10. CONCLUSIONS 46

11. ACKNOWLEDGMENTS 47

12. REFERENCES 47

LIST OF TABLES

Table 1. Composition of 20% chromium alloys 3

Table 2. Intermetallic phases observed in 20/25% chromium alloys 7

Table 3. Carbide, nitride, and phosphide phases observed in 20/25% chromium alloys 10

Table 4. Summary of welding technology for 20/25% Cr alloys 24

Table 5. Tensile data for HT-UPS alloys 31

Table 6. Summary of creep-rupture data on HT-UPS alloys 33

Table 7. Tensile data for HT-UPS alloy weldments 43

Table 8. Stress-rupture of weldments in HT-UPS alloys 44

LIST OF FIGURES

Fig. 1. Location of several alloys in the iron-nickel-chromium ternary phase diagram at 650°C 5

Fig. 2. Comparison of the room-temperature stress versus strain curves of the AX series, HT-UPS alloys. Anneals include 1115 and 1200°C and MA (mill anneal) that involved 1200°C plus 10% cold roll of plate 9

Fig. 3. TEM of the microstructure developed in AX2 after 12,500 h at 700°C and 170 MPa. Fine MC particles appear in dislocation tangles and a few large MC are present in the TEM 11

Fig. 4. Effect of aging at 700°C for 10,000 h on the creep curves of AX3 at 700°C. 13

Fig. 5. Creep curves for AX series alloys at 700°C and 170 MPa: (*a*) mill anneal condition–1,200°C anneal plus 10% cold roll and (*b*) 1,200°C anneal 15

Fig. 6. Photomicrographs of the microstructures of mill anneal AX alloys: (*a*) AX1, (*b*) AX2, (*c*) AX3, and (*d*) AX4 17

Fig. 7. Photomicrographs of HT-UPS tubing: (*a*) CET2 and (*b*) BWT. 19

Fig. 8. Coextruded HT-UPS alloy tubing—alloy 690 on BWT. 22

Fig. 9. Weld overlay and roll-clad HT-UPS plate: (*a*) alloy 690 on BWT and (*b*) alloy 672 on BWT 23

Fig. 10. Photomicrographs showing HAZ cracking in AX series alloys produced in welds with 17-14CuMo stainless steel filler metal: (*a*) AX1 with 0.07% P, (*b*) AX2 with 0.045% P, (*c*) AX3 with 0.03% P, and (*d*) AX4 with 0.07% P 25

Fig. 11. Photomicrograph of weld region in cold-rolled BWT plate welded with alloy 556. 27

Fig. 12 Photomicrographs of weld region in annealed BWT plate welded with alloy 556. 27

Fig. 13. Yield and tensile strengths versus temperature for several alloys (*a*) alloy 800H, (*b*) NF709 stainless steel, (*c*) HR3C stainless steel, and (*d*) 253MA stainless steel 30

Fig. 14. Yield and tensile strengths versus temperature for HT-UPS alloys. 31

Fig. 15. Log stress versus the Larson-Miller parameter for rupture based on typical strengths at 1,000 and 10,000 h for four alloys: (*a*) alloy 800HT, (*b*) NF709 stainless steel, (*c*) HR3C stainless steel, and (*d*) 253MA stainless steel 34

Fig. 16. Log stress versus the Larson-Miller parameter of rupture of HT-UPS alloys: (*a*) mill-annealed AX series, (*b*) 1200°C annealed material, and (*c*) lower temperature-annealed material 35

Fig. 17. Ductility versus rupture life for HT-UPS alloys: (*a*) elongation and (*b*) reduction of area 38

Fig. 18. TEM of HT-UPS alloy AX2 showing regions of recovery/ recrystallization after 12,500 h at 700°C and 170 MPa 39

Fig. 19. Performance of candidate tubing alloys tested by Van Weele and Blough under coal ash corrosion conditons 46

EVALUATION OF ADVANCED AUSTENITIC ALLOYS RELATIVE TO ALLOY DESIGN CRITERIA FOR STEAM SERVICE - PART 2 - 20 to 30% CHROMIUM ALLOYS

R. W. Swindeman and P. J. Maziasz

ABSTRACT

The results are summarized for a task within a six-year activity to evaluate advanced austenitic alloys for heat recovery systems. Commercial, near-commercial, and developmental alloys were evaluated relative to criteria for metallurgical stability, fabricability, weldability, mechanical properties, and corrosion in fireside and steamside environments. Alloys that were given special attention in the study were 800HT®, NF709®, HR3C®, and a group of 20/25% chromium-30% nickel-iron alloys identified as HT-UPS (high-temperature, ultrafine-precipitation strengthened) alloys. Excellent metallurgical stability and creep strength were observed in the NF709 and HR3C steels that contained niobium and nitrogen. One group of HT-UPS alloys was strengthened by solution treating to temperatures above 1150 °C and subsequent cold or warm working. Test data to beyond 35,000 h were collected. The ability to clad some of the alloys for improved fireside corrosion resistance was demonstrated. Weldability of the alloys was a concern. Hot cracking and heat-affected-zone (HAZ) liquation cracking were potential problems in the HR3C stainless steel and HT-UPS alloys, and the use of dissimilar metal filler wire was required. By the reduction of phosphorous content and selection of either a nickel-base filler metal or alloy 556 filler metal, weldments were produced with minimum HAZ cracking. The major issues related to the development of the advanced alloys were identified and methods to resolve the issues suggested.

---

1. INTRODUCTION

An assessment by Rittenhouse et al. (1985) of the materials needs related to the development of advanced steam cycle coal-fired power plants identified several materials selection issues that could be addressed by research supported by the U.S. Department of Energy Advanced Research and Technology Development (AR&TD) Fossil Energy Materials Program. One issue was the choice of an alloy for the superheater/reheater where high-strength, corrosion-resistant tubing is required. The alloy design and evaluation methods for this application were then specified by Swindeman et al. (1986) in ORNL-6274, and a

*Research sponsored by the U.S. Department of Energy, Office of Fossil Energy, Advanced Research and Technology Development Materials Program [DOE/FE AA 15 10 10 0, Work Breakdown Structure Element ORNL-2(B)] under contract No. DE-AC05-84OR21400 with Martin Marietta Energy Systems, Inc.

six-year activity was started to examine the potential of commercial, near-commercial, and developmental alloys. The alloys were separated into four categories: lean stainless steels containing less than 20% chromium; high-chromium, high-nickel, iron-based alloys containing 20 to 30% chromium and 20 to 30% nickel; nickel-based alloys for cladding; and aluminum-bearing alloys. Because of their strength potential and relatively low cost, emphasis was initially placed on the performance of lean stainless steels, and Part 1 of this report summarized the status of that research (Swindeman et al. 1990). Several university and industrial subcontractors were involved in the work, and their results on the higher chromium alloys have reached a stage where the information may be folded into the data produced at the Oak Ridge National Laboratory (ORNL) to form a fairly comprehensive picture of the strengths and weaknesses of this group of alloys. Specifically, Topolski (1991) has finished work on the fabrication technology; Ferro et al. (1990) have completed studies of the high-temperature, ultrafine-precipitation strengthened (HT-UPS) alloys in regard to optimization of thermal-mechanical processing; Lundin et al. (1989) have assessed weldability; and Blough and Van Weele (1991) have completed the first round of fireside corrosion studies.

The information provided in this report addresses the evaluation of the 20/25% Cr-20/30% nickel-iron alloys relative to the alloy design criteria specified in ORNL-6274 (Swindeman et al. 1986). The criteria were divided into five categories: metallurgical stability, fabrication and joining, mechanical properties, fireside corrosion, and steamside corrosion. There exists an overlap between these categories, but an attempt is made in the information that follows to retain the framework identified in the alloy design criteria report. Some of the criteria required to assure satisfactory performance of the lean stainless steels were not needed for the higher chromium alloys and were eliminated from consideration here.

2. MATERIALS

Several 20 to 30% chromium austenitic alloys are viable candidates for superheater/reheater tubing in an advanced steam cycle. The development and performance of these alloys for the advanced steam cycle applications have been reviewed recently by Viswanathan (1989), so a relatively complete and current evaluation is available in the literature.

Compositions to be discussed in this report are listed in Table 1. Included in the first group of alloys are those that are used on a commercial basis in the United States and identified in Sect. I of Sect. II of the American Society of Mechanical Engineers (ASME) Boiler and Pressure Vessel (BPV) Code. These alloys include type 310 stainless steel, alloy 800HT®, and 253MA® stainless steel. All of these alloys are relatively weak and are not considered

Table 1. Composition of 20/25% chromium alloys

Alloy	C	Si	Mn	Ni	Cr	Ti	Nb	V	Mo	P	B	S	N	Al	Other
253MA	0.080	1.70	0.60	11.1	21.1					.04 max		.03 max	0.170		0.04 Ce
800H	0.080	0.24	0.90	32.1	20.1	0.42				.04 max				0.43	
800HT	0.080	1 max	1.5 max	32.1	21.1	0.6**				.04 max		.015 max		0.6*	
310SS	0.080	0.60	1.60	20.1	25.1										
NF709	0.150	0.50	1.00	25.1	20.1		0.20		1.50		0.005		0.050		
HR3C	0.060	0.40	1.20	20.1	25.1		0.45						0.200		
m800	0.080	0.40	0.80	34.1	22.1		0.40		1.25						
HR-120	0.050	0.60	0.70	37.1	25.1	0.10	0.70		2.50		0.004		0.200	0.10	2.5W
AX1	0.087	0.20	1.99	30.1	20.1	0.27	0.21	0.52	1.98	0.074	0.005	0.012	0.030		
AX2	0.090	0.23	1.96	30.1	20.1	0.36	0.24	0.53	1.96	0.045	0.011	0.009	0.028		
AX3	0.092	0.22	2.00	31.1	21.1	0.36	0.24	0.52	2.00	0.031	0.010	0.010	0.029		
AX4	0.091	0.22	1.97	30.1	25.1	0.36	0.24	0.53	1.97	0.072	0.011	0.009	0.030		
CET2	0.095	0.24	1.93	31.1	21.1	0.29	0.20	0.47	1.99	0.003	0.007	0.013	0.010	0.02	
BWT7	0.100	0.19	2.00	30.1	20.1	0.28	0.22	0.59	1.89	0.020	0.006	0.006	0.007	0.01	

*Combined Ti + Nb must be 1.2% or greater.

adequate to meet the specified design criteria for superheater tubing steam at 650°C, 35 MPa. A second group of alloys in Table 1 covers near-commercial alloys and includes Nippon Steel NF709® stainless steel (Takahashi et al. 1989) and Sumitomo HR3C® stainless steel (Yoshikawa et al. 1989). These alloys are considered to be the prime candidates for advanced steam cycle superheater tubing. The third group of alloys is comprised of new materials that are in the research stage. Alloys include Hitachi-modified 800H (Doi et al. 1988), alloy HR-120® (Haynes Alloys 1989), and variations within an alloy family identified as HT-UTS steels by Maziasz (1989), which are modifications of alloy 800H. Alloy HR-120 is very new and will not be evaluated in this report.

The chemistries of the alloys listed in Table 1 should be regarded as typical and do not provide the range specified for the specific alloy designation. The fabrication procedures, heat treatments, and important processing variables are provided in the appropriate sections included below and in the appendices.

3. METALLURGICAL STABILITY

The alloy design criteria in ORNL-6274 specified that stability would be assured by the suppression of intermetallic and other embrittling phases through the addition of elements that promote austenitic stabilization. Means of accomplishing this objective have been reviewed by Maziasz (1987 and 1989) and will not be discussed here in any detail. Addressing the specific alloy design criterion listed in ORNL-6274, the findings below are pertinent:

<u>I-A. The alloys will fall within or near the austenite field of the iron-nickel-chromium ternary diagram at temperatures in the range of 500 to 750°C.</u>

To meet this criterion for a temperature of 650°C, the alloys need to have equivalent chromium and nickel levels that place them near the γ field of the iron-nickel-chromium phase diagram provided in Fig. 1. In their reviews, Harries (1982) and Marshall (1984) plotted the iron-nickel-chromium ternary phase diagram for several temperatures. They used the following formulae for the nickel and chromium equivalents:

$$Ni_{eq}(A) = Ni + Co + 0.5\ Mn + 30\ C + 0.3\ Cu + 25\ N \tag{1}$$

and

$$Cr_{eq}(A) = Cr + 2\ Si + 1.5\ Mo + 5\ V + 5.5\ Al + 1.75\ Nb + 1.5\ Ti + 0.75\ W\ , \tag{2}$$

ORNL-DWG 90-8145

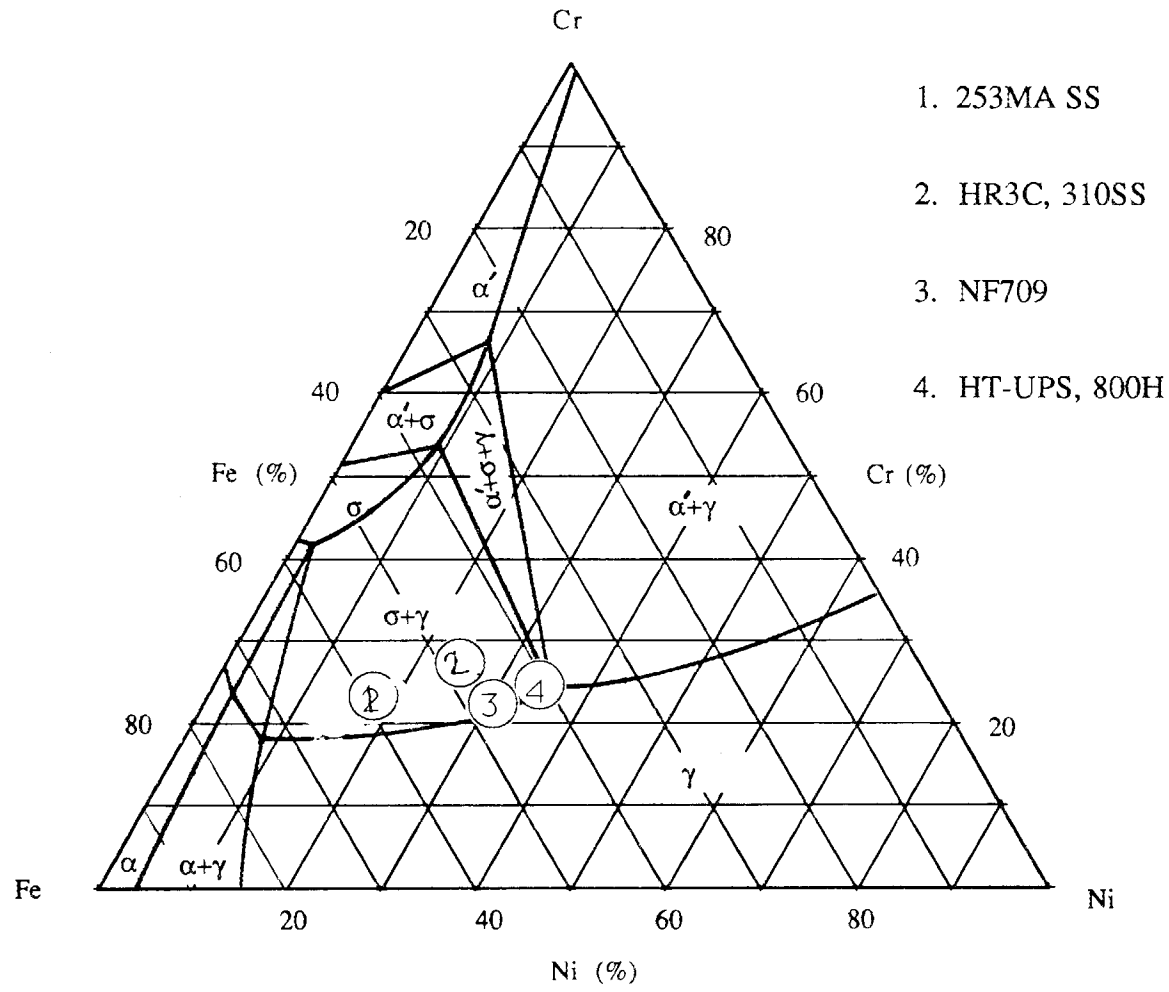

Fig. 1. Location of several alloys in the iron-nickel-chromium ternary phase diagram at 650°C.

where the weight percent of each of the indicated elements is used in the formulae. Data provided in Table 1 were used in combination with the equations above to determine the locations of several alloys within the ternary diagram shown in Fig. 1. Virtually all alloys fell into the austenite plus sigma field that occurs at 650°C. However, the use of Eqs. (1) and (2) to locate alloys in the ternary diagram did not take into consideration the fact that carbide and nitride precipitates deplete the matrix of elements that stabilize austenite (such as carbon and nitrogen) or promote sigma phase (such as molybdenum and niobium). The HR3C alloy falls well within the alpha plus sigma field, and some sigma phase has been found by Yoshikawa et al. (1989). However, the sigma phase was sparsely distributed and was not detrimental to the alloy performance. All of the developmental alloys listed in Table 1 were judged to be sufficiently close to the austenite field at 650°C to meet criterion I-A.

I-B. The chromium and nickel equivalents will be maintained to balance the matrix composition on the high-nickel equivalent side.

Several empirical equations have been developed that use the terms "nickel equivalent" and "chromium equivalent." Equations (1) and (2) were provided in connection with the ternary phase diagram. Similar terms are used in connection with fabricability, weldability, and long-term metallurgical stability, and these terms were reviewed by Ellis et al. (1988) and Domian and LeBeau (1989) in connection with their assessment of the fabricability of the lean stainless steels. In specifying criterion I-B, the equations used for $Ni_{eq}(B)$ and $Cr_{eq}(B)$ were based on the DeLong (1974) equations written as

$$Ni_{eq}(B) = Ni + 0.5\ Mn + 30(C+N) \tag{3}$$

and

$$Cr_{eq}(B) = Cr + Mo + 1.5\ Si + 0.5\ Nb\ . \tag{4}$$

On the basis of these two equations, only type 310 stainless steel and 253MA were balanced on the high $Cr_{eq}(B)$ side. Domian and LeBeau found the HT-UPS alloys to be balanced toward austenite.

I-C. Local chemical changes associated with the depletion of austenite-stabilizing elements will not produce excessive sigma and Laves.

The phases present in several of the alloys have been identified and reported in the literature. Some information has been provided in Table 2. First, minor compositional

Table 2. Intermetallic phases observed in 20/25% chromium alloys

Alloy	Phases	Reference
800H	Gamma prime	Villagrana et al. 1978 Tavassoli and Colombe 1978 Maziasz 1989
310 SS	Sigma	Menard 1952
NF709	None	
HR3C	Sigma	Sawaragi et al. 1986
m800	None	Doi et al. 1986
AX2/AX3	Laves	Maziasz 1989
AX4	None	

differences, thermal-mechanical condition, and time-temperature-stress conditions influence the kinetics and location of sigma, Laves, and gamma prime phase formation. Not all intermetallic phases are present at the same time, nor do they occur in the same location within the microstructure or produce the same embrittlement. Large amounts of sigma and Laves are undesirable. Massive sigma phase has been observed in type 310 stainless steel (Menard 1952), but the amount diminishes as silicon content is reduced (Payson and Savage 1947). Small amounts of blocky sigma phase were observed in HR3C stainless steel as mentioned earlier. Little is known about intermetallic phases in NF709 and 253MA.

Alloy 800HT formed gamma prime (Villagrana et al. 1978 and Tavassoli and Colombe 1978), but no sigma and Laves phases have been reported. The Hitachi-modified 800H was free from intermetallics (Doi et al. 1986). The HT-UPS alloys that have been examined revealed small amounts of both sigma phase, Laves phase, and phosphides (Maziasz 1989).

The amount of precipitation as a function of time has yet to be modeled for the high-strength alloys containing nitrogen and niobium. Qualitatively, information available suggests that the weight percent of intermetallic phases will vary with small differences in chemical composition and thermal-mechanical treatment, but evidence suggests that the small amount of intermetallic phases produced at temperatures in the range of 600 to 760°C will not produce embrittlement problems.

I-D. The alloys will be strengthened by solid solution elements and by the development of carbides and carbonitrides.

Attempts have been made to correlate solid solution strengthening of austenitic iron-based alloys with composition. Examples of correlations of composition with short-time properties may be seen in the work of Pickering (1979) and Irvine et al. (1969). The correlation of ultimate tensile strength (UTS) with chemistry has been given by Irvine et al. (1969) as

$$UTS = 15.4(29 + 35\,C + 55\,N + 2.4\,Si + 0.11\,Ni + 1.2\,Mo + 5\,Nb + 3\,Ti + 1.2\,Al + 0.82\,t^{-1/2}), \quad (7)$$

where UTS is in MPa, the elements are in weight percent, and t is twin spacing in millimeters. In addition to carbon and nitrogen, the "advanced" alloys listed in Table 1 contain important solution hardening elements such as molybdenum, niobium, and titanium. Vanadium is not included in Eq. (7) but should increase strength as well. Nitrogen was specifically added to HR3C to increase the yield and tensile strengths and a significant amount remained in solution after long-time exposure (Sawaragi et al. 1988 and Yoshikawa et al. 1989). Several levels of nitrogen were investigated in regard to NF709, and higher yields and ultimate strengths corresponded to higher nitrogen levels (Takahashi et al. 1989). The nitrogen addition to HR3C, NF709, and 253MA stainless steels raised the yield and ultimate strengths quite nicely, and minimum strengths for annealed tubing were well in excess of 300 MPa for all three alloys.

It was expected that some of the candidate alloys without nitrogen additions would be amenable to thermal-mechanical treatments to optimize their short-time strength beyond that expected from the solid solution hardening. By cold or warm working, for example, the yield strengths of the MC-forming alloys could be raised to levels where advantage could be taken of their extraordinary creep-rupture strength at temperatures where the minimum yield or tensile strength would ordinarily limit the allowable design stress intensity. Cold or warm work was required to raise the yield strength of alloy 800HT and the HT-UPS alloys, and an example of the influence of annealing temperature and cold work is shown in Fig. 2. The stress versus strain curves are shown from tensile tests at room temperature for alloy 800H and the four AX series alloys. Yield strengths for specimens annealed at 1200°C were well below 300 MPa, but the AX series alloys with more solution strengthening additions were clearly stronger than alloy 800H. A mill-annealed condition, which involved 10% reduction of thickness after the 1200°C anneal, increased the yield strength to values above 400 MPa.

ORNL-DWG 90-17185

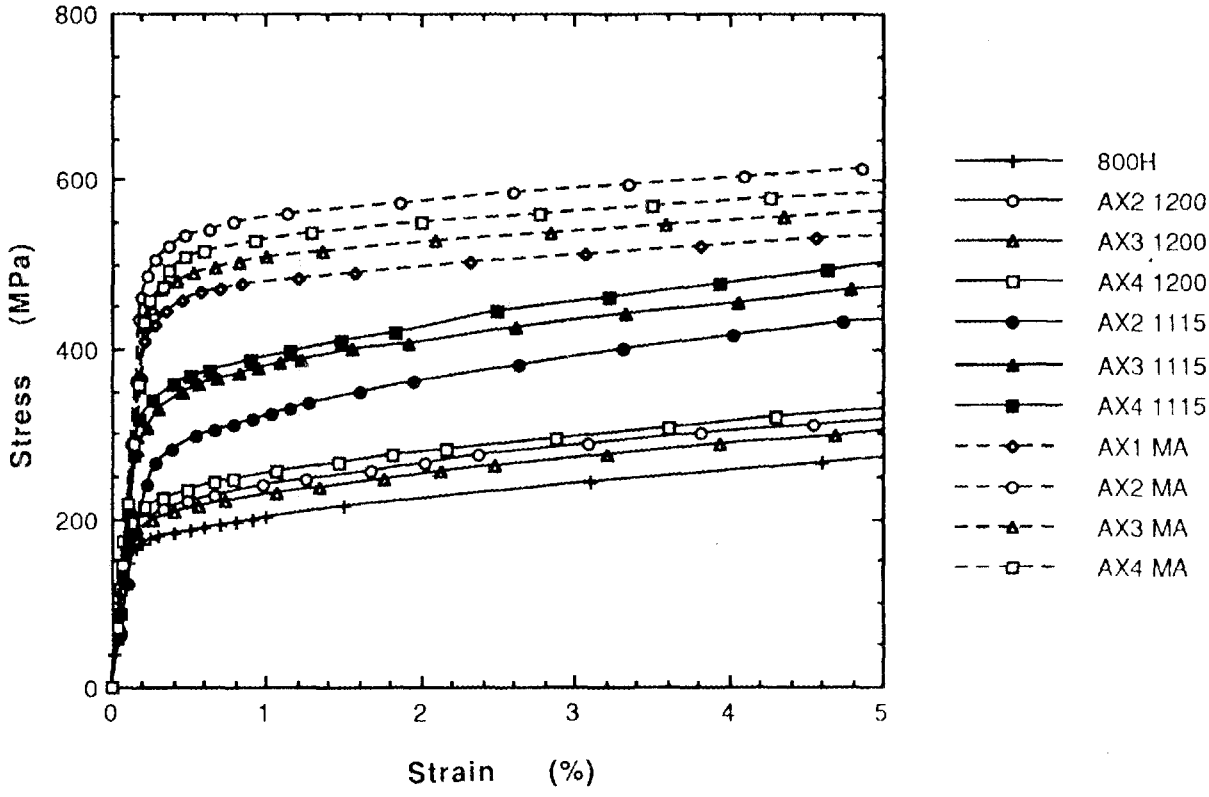

Fig. 2. Comparison of the room-temperature stress versus strain curves of the AX series, HT-UPS alloys. Anneals include 1115 and 1200°C and MA (mill anneal) that involved 1200°C plus 10% cold roll of plate.

Creep strength was developed in the alloys by means of the precipitation of second phases. All of the alloys developed carbide precipitates during exposure at temperatures in the range of interest to advanced steam cycle applications (550 to 750°C). Some alloys developed nitrides and carbonitrides. The types of carbides that have been observed are provided in Table 3. The high-temperature creep strength was largely controlled by the size, spacing, and stability of these precipitates, both within the grains (matrix strengthening) and in the grain boundaries (grain boundary strengthening). Precipitates typically included two types of carbides ($M_{23}C_6$ and MC), a nitride (NbCrN), a phosphide (MP) phase designed into some of the HT-UTS alloys by Maziasz (1988), and gamma prime, which precipitated in alloy 800H (Villagrana et al. 1978). The precipitation, dissolution, and changes of the elemental compositions of these precipitates are very complex phenomena, and it is well beyond the scope of this report to provide a comprehensive picture for the alloys. The criterion that the alloys be strengthened by precipitates was originally intended to allow this mechanism to be

Table 3. Carbide, nitride, and phosphide phases observed in 20/25% chromium alloys

Alloy	Phases	References
800H	$M_{23}C_6$, MC, MN, M(CN), MP	Villagrana et al. 1978 Tavassoli and Colombe 1978 Maziasz 1989
310 SS	$M_{23}C_6$	Menard 1952 Payson and Savage 1947
NF709	$M_{23}C_6$, M(CN)	Takahashi et al. 1989
HR3C	$M_{23}C_6$, M(CN)	Sawaragi et al. 1986
m800	$M_{23}C_6$, MC	Doi et al. 1986
AX2/AX3	$M_{23}C_6$, MC, MP	Maziasz 1989
AX4	$M_{23}C_6$, MP	Maziasz 1989

designed into the alloys, rather than excluded. The thermal-mechanical treatments that optimize the strength and ductility, however, were expected to vary significantly from one alloy to the next.

In all alloys, the $M_{23}C_6$ precipitate quickly formed on grain boundaries at the temperatures of interest to the advanced steam cycle and formed within the matrix at a rate that depended on a number of complicating factors. The $M_{23}C_6$ carbide was reported to be the strengthening phase in HR3C, NF709, and 800HT and formed in only a few hours at temperatures above 650°C. The MC carbide developed early but was replaced in the HR3C and NF709 alloys by $M_{23}C_6$.

In alloy 800H, the MC carbide was present in small quantities and its appearance was not influenced by cold working in the range of 5 to 10% (Villagrana et al. 1978). In contrast, the HT-UPS alloys developed MC precipitates quickly, and cold work accelerated and improved the distribution as it provided nucleation sites energically favorable for the formation (Maziasz 1988). A typical transmission electron micrograph (TEM) is shown in Fig. 3, which reveals the general character of the precipitates in the AX2 alloy after long-time creep exposure at 700°C.

Fig. 3. TEM of the microstructure developed in AX2 after 12,500 h at 700°C and 170 MPa. Fine MC particles appear in dislocation tangles and a few large MC are present in the TEM.

In the course of research on the HT-UPS alloys, a wide variety of thermal-mechanical treatments was examined by Ferro et al. (1990). They found that solution treating in the temperature range of 1150 to 1200°C, followed by 2 to 5% cold work and aging at temperatures in the range of 800 to 850°C, produced the best combination yield and creep strengths. However, some of the HT-UPS alloys showed greater response to thermal-mechanical treatment than others. The AX series alloys, for example, were strengthened to a greater degree than the CET2 alloy. Ferro et al. (1990) traced some of the differences to grain size effects, with coarse grain size being better for improved creep resistance.

None of the alloys required aging treatments to develop strength prior to creep testing, and evidence collected to date suggests that Criterion I-D can be met for the near-commercial and developmental alloys.

I-E. Aging due to Ostwald ripening will not degrade short-time strength below the minimum specified for starting material.

Ostwald ripening is a phenomenon in which the precipitate particles become fewer in number and larger in size as a result of long-time exposure at temperatures where diffusion is significant. Alloys that depend on precipitate strengthening to meet short-time strength requirements could lose strength as a result of Ostwald ripening. Alloys that depend on precipitates for long-time strength could degrade in service.

The purpose of Criterion I-E was to assure that coarsening of precipitates would not result in a significant softening of an alloy whose strength depended on pre- or in-service age hardening. Aging of austenitic stainless steels has been a subject of research for decades, and much is known about type 310 stainless steel and alloy 800H. Aging of NF709 stainless steel was completed for several thousand hours at 700°C by Takahashi et al. (1989), and aging of HR3C stainless steel at temperatures from 600 to 800°C was examined by Yoshikawa et al. (1988). As a rule, the room-temperature yield and ultimate strengths of these solution-treated alloys increased with time due to carbide or nitride precipitation. Some loss in tensile ductility was noted, but this was generally attributed to the formation of grain-boundary carbides rather than age softening due to Ostwald ripening of precipitates.

Microstructural effects on aging of Hitachi-modified 800H at 700°C were examined by Doi et al. (1986). They found the precipitate structure to develop quickly and stabilize for at least 3,000 h.

Aging response of alloy 800H was examined by Villagrana et al. (1978) and Tavassoli and Colombe (1978). They found an increase in strength that depended on the alloy composition and an overaging effect. Some heats of 800H exhibited overaging behavior in regard to hardness.

A systematic study of the aging characteristics of the HT-UPS alloys has yet to be undertaken. One alloy, cold-rolled AX3, was tested after aging 10,000 h at 700°C. It was found that the room-temperature yield strength remained the same while the ultimate strength increased slightly. The short-time creep strength was also degraded by the aging. Typical creep curves for tests at 700°C are shown in Fig. 4.

Insufficient evidence exists to assure that Criterion I-E can be met for all alloys. However, the long-time data available for the HR3C and NF709 stainless steels are good indicators that these alloys will perform satisfactorily.

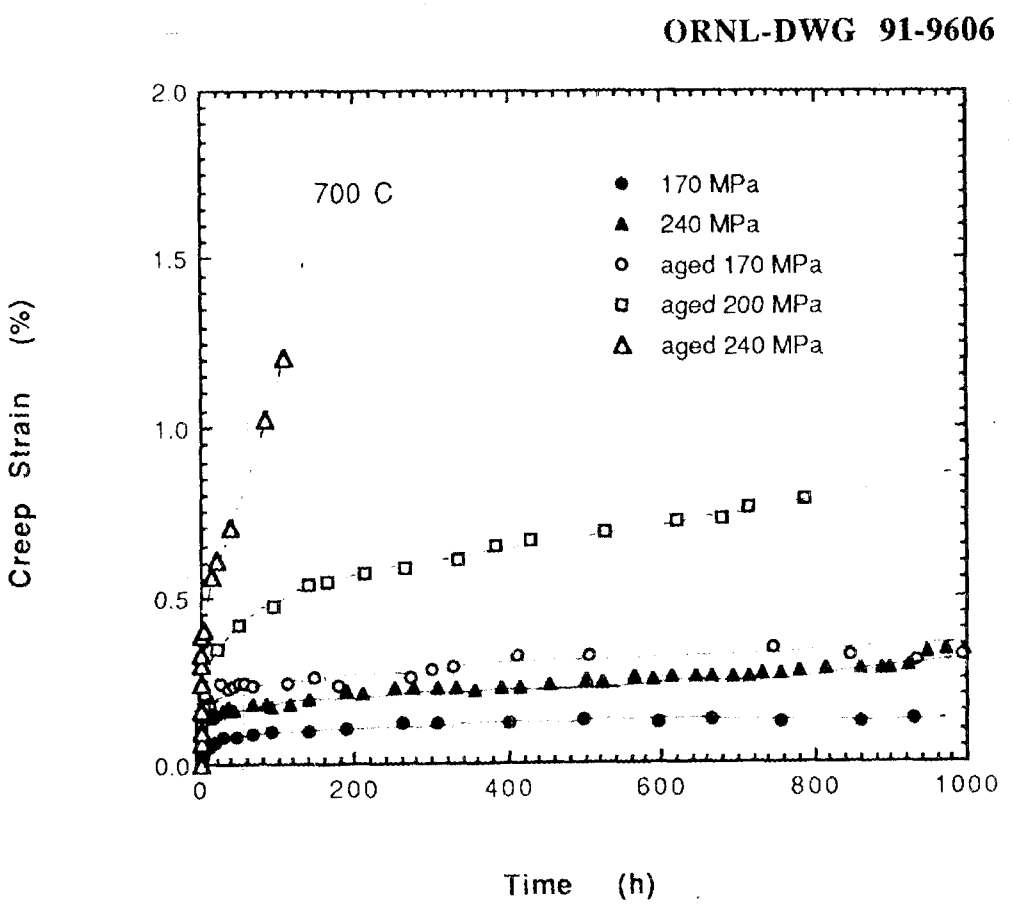

Fig. 4. Effect of aging at 700°C for 10,000 h on the creep curves of AX3 at 700°C.

I-F. The alloys will have a tolerance for at least 15% cold work introduced during boiler fabrication.

Cold-worked alloys have been avoided in high-temperature applications by much of the BPV industry. Small levels of cold work in alloy 800H were known to produce low ductility creep-rupture failures (Smith 1978), while high levels of cold work could promote recrystallization during service. However, the MC- and MN-forming alloys benefit greatly from cold work, since the dislocations produced by cold or warm work promote and stabilize the formation of fine carbide and nitride dispersions. These dispersions led to a fine $M_{23}C_6$ dispersion in NF709 and HR3C stainless steel.

Ferro and coworkers (1990) made an effort to establish the optimum thermal-mechanical treatment for the HT-UPS alloys. They examined cold work in the range of 1 to 5% and noted improvement in relaxation strength at temperatures in the range of 650 to 760°C. In no instances did they observe a loss in strength of cold-worked and aged materials (relative to annealed material) that would indicate recrystallization under relaxation conditions.

Cold work did not appear to be deleterious to creep-rupture strength of the HT-UPS alloys. For example, all the AX alloys had greater rupture lives in the 10% cold-rolled condition than after annealing at 1200°C. Comparisons are made in Fig. 5. Cold rolling lowered the creep strain at which tertiary creep started, however, and this aspect required consideration and further evaluation by long-time testing.

All evidence suggests that the near-commercial and developmental alloys should tolerate cold work at levels to 10%. Insufficient data are available to confirm compliance to the tolerance for 15% cold work specified in Criterion I-H.

4. FABRICATION AND JOINING

The general criterion that governed the fabrication and joining requirements for the advanced steam cycle alloys was that production methods be typical of good fabrication practices in the boiler tubing industry. The commercial and near-commercial alloys listed in Table 1 have been produced as tubing, and some alloys (e.g., HR3C and NF709 stainless steels) have had years of boiler exposure at conditions almost as severe as what might be expected in the advanced steam cycle under consideration here. Less is known about the HT-UTS alloys; hence, they will receive most of the attention in this section.

ORNL-DWG 91-9607

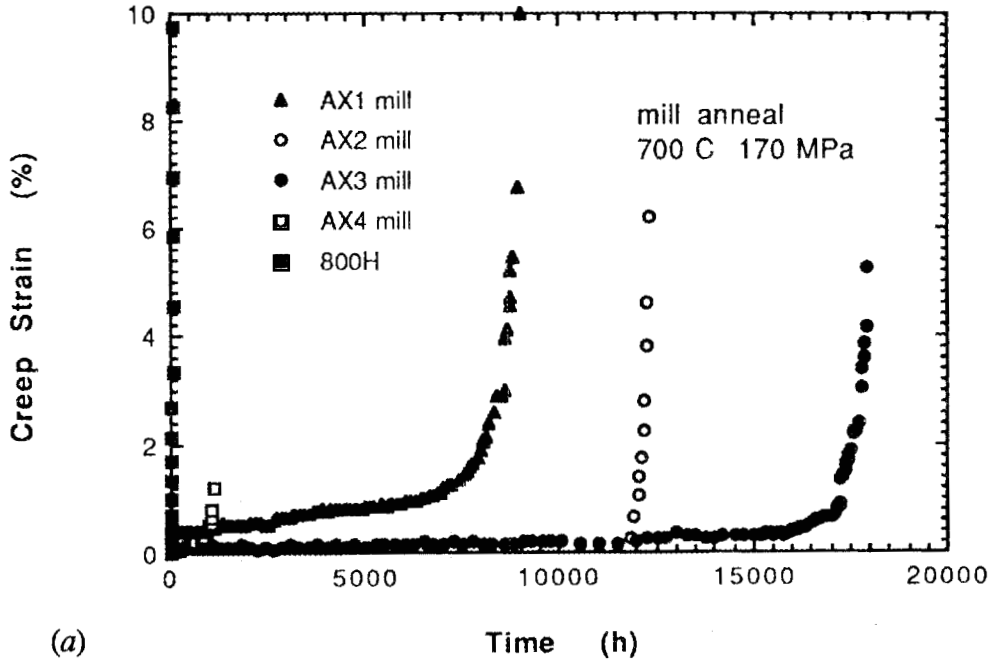

(*a*)

ORNL-DWG 91-9608

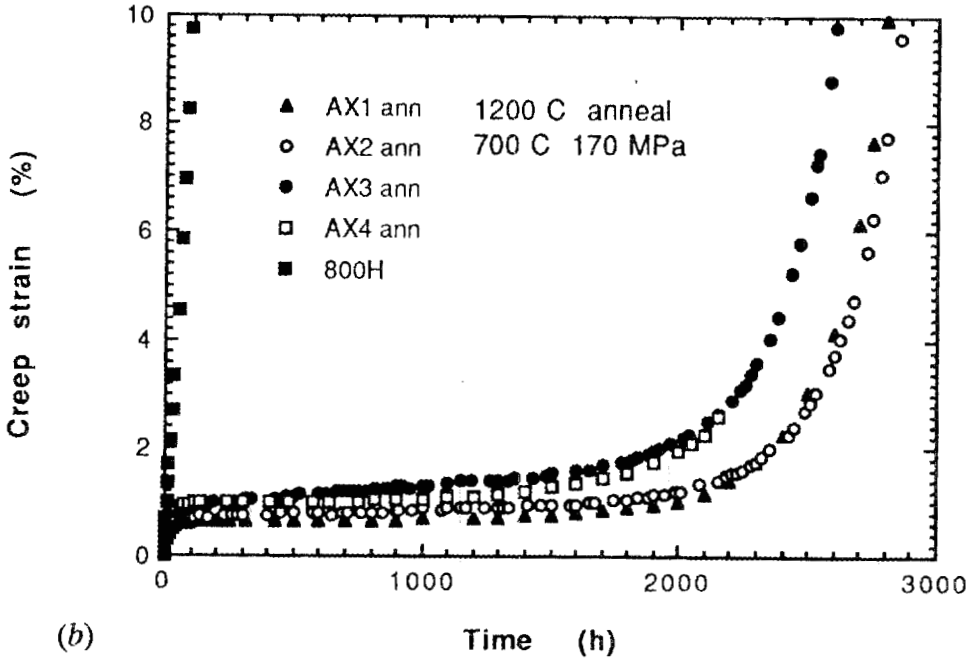

(*b*)

Fig. 5. Creep curves for AX series alloys at 700°C and 170 MPa: (*a*) mill anneal condition–1200°C anneal plus 10% cold roll and (*b*) 1200°C anneal.

II-A. The alloys will be capable of meeting American Society for Testing and Materials (ASTM) A 213 for the production of seamless tubing.

The literature review undertaken by Domian and LeBeau (1989) to evaluate the behavior of the HT-UPS alloys regarding melting practice, workability, and phase stability identified several possible tube-making routes, all of which required hot working of cast and wrought structures in the temperature range of 1000 to 1200°C, followed by cold working. The hot workability was assessed on the basis of the ratio of a nickel equivalent to a chromium equivalent that was proposed by Myllykosi (1983). These equivalencies are different than those previously given but involve several of the same alloying elements

$$Ni_{eq}(C) = Ni + 0.31\ Mn + 22\ C + 14.2\ N + Cu \tag{8}$$

and

$$Cr_{eq}(C) = Cr + 1.37\ Mo + 1.5\ Si + 2\ Nb + 3\ Ti\ , \tag{9}$$

where all elements are in weight percent. The optimum workability of the cast structure is achieved with the ratio $Cr_{eq}(C)/Ni_{eq}(C)$ around 1.5. Lower values of the ratio represent potential cracking problems due to impurity element embrittlement on austenite grain boundaries, while higher values of the ratio portend cracking problems at austenite/ferrite interfaces. Domian and LeBeau (1989) reached several conclusions regarding the workability of the HT-UPS alloys. They found them to be fully austenitic and prone to hot cracking in both working and welding processes. They suggested that the melting practice be selected to produce a low residual element content (Pb, As, Bi, S, Sb, and Sn). They suggested that rare earths be added to improve resistance to hot cracking.

The heats of HT-UTS alloys were manufactured by various fabrication routes. The first group of alloys (AX1 through AX4) was produced by the AMAX Company. The alloys were argon-induction melted, poured as 20-kg ingots, and homogenized at 1250 °C. The surfaces of the ingots were machined, and rolling was performed at 1100°C (with 10% reduction of thickness per pass) and 1200°C annealing between passes. The final rollings were cold with approximately 10% reduction in thickness to produce final thicknesses of 13 mm. High yields were obtained with nearly all of the cropped and machined ingot being usable. Photomicrographs of the mill-annealed AX alloy microstructures are provided in Fig. 6 for alloys AX1 through AX4. There was no evidence of cold work in the photomicrographs, and virtually the same microstructures were observed in the specimens reannealed at 1200°C.

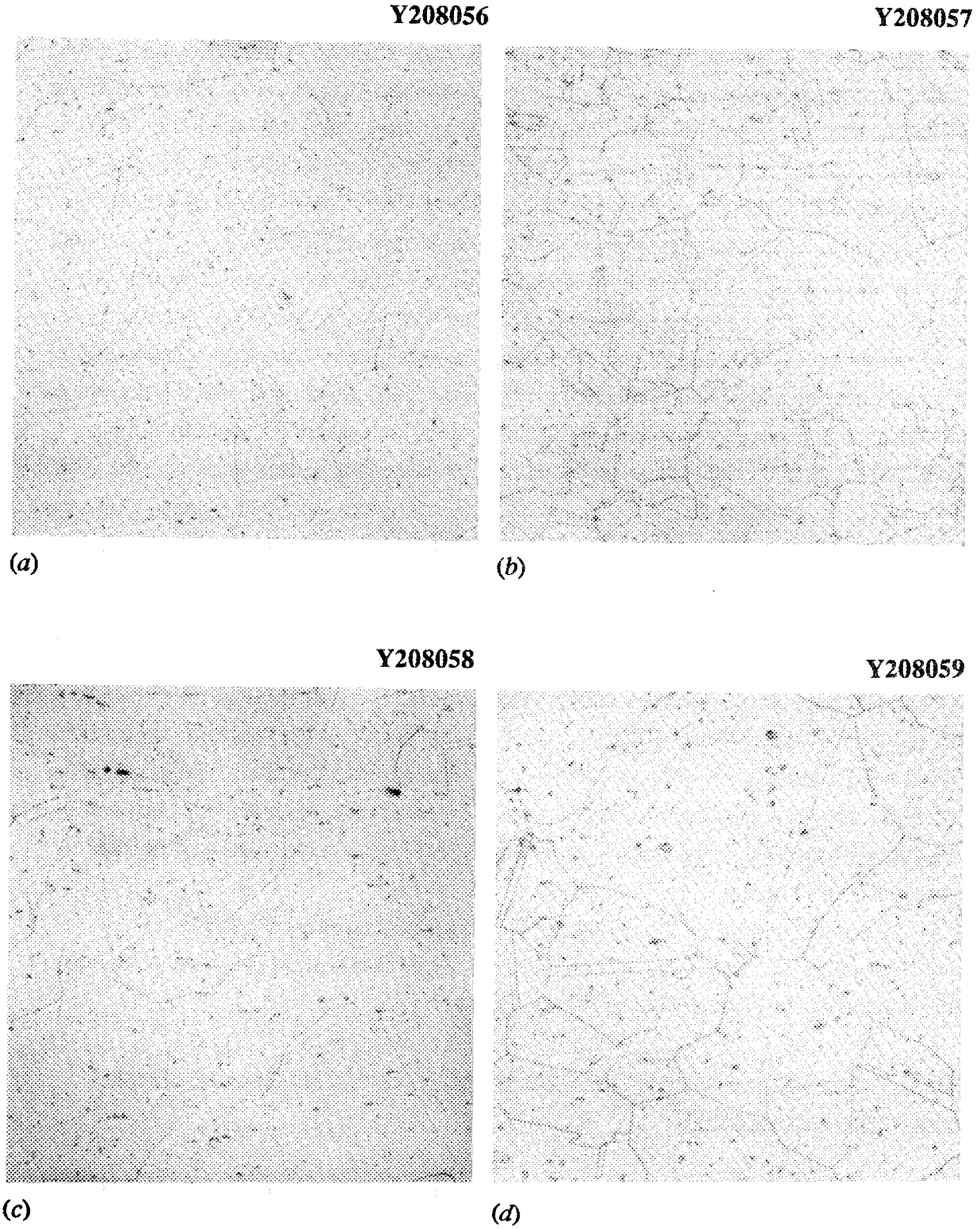

Fig. 6. Photomicrographs of the microstructures of mill anneal AX alloys: (*a*) AX1, (*b*) AX2, (*c*) AX3, and (*d*) AX4.

CET2 was tubing produced by a melting and forming practice that involved centrifugal casting and cold pilgering. This process most closely conformed to commercial boiler tube manufacturing practices and was performed by Combustion Engineering. The production sequence involved argon-induction melting and centrifugally casting a tube hollow 130 mm in diameter, 29 mm in wall thickness, and 3 m in length. The tube hollow was then homogenized at 1175°C for 1 h, water quenched, machined to 120-mm OD by 19-mm thickness, and cold pilgered in a two-pass operation with an intermediate anneal at 1175°C. The final anneal was at 1125°C. The tubing was rotary straightened and ultrasonically inspected. Approximately 5 m of sound tubing was produced with dimensions of 63-mm diam. and 6.9-mm thickness. A problem was encountered in regard to the centrifugal casting of the titanium-bearing alloy. This involved the oxidation of titanium on the inside diameter of the casting, which produced oxide islands. Machining of the inside diameter of the tubing removed much of the oxide, but in order to meet the target tubing dimension with the available tooling, it was necessary to leave regions that included significant oxide islands. These were carried through the subsequent fabrication processes and caused the rejection of at least 50% of the tubing on the basis of defects penetrating more than 10% of the wall thickness. The microstructure is shown in Fig. 7(*a*) .

The production of the BWT7 alloy listed in Table 1 was described in detail by LeBeau (1990) and Topolski (1991). The alloy was vacuum-induction melted and electroslag remelted at Tedyne Allvac to produce a 1270-kg, 330-mm-diam ingot. Approximately one-half of the ingot was forged to a 150-mm-diam billet, surface conditioned, drilled, and extruded by AMAX Corporation using standard practices. Several tubes were produced, each 4 m in length, 63-mm diam, and 13-mm wall thickness. Additional tubing was cold finished to produce 50-mm tubing with 7.5-mm wall.

The microstructure of the extruded BWT7 tubing is provided in Fig.7(*b*).

Assuming that melting practices would be selected that avoided excessive oxidation of titanium, it appears that all alloys can meet Criterion II-A.

<u>II-B. Tubing will be suitable for service in the mill-annealed condition after solution temperatures above 1100°C.</u>

The advanced alloys listed in Table 1 contain MC-forming elements and are typically solution treated at 1100°C or higher. Generally speaking, the Nb-bearing alloys should be solution treated above 1150°C, with temperature increasing with niobium content (Keown and Pickering 1972). The "mill-annealed" condition assures that the alloy has been solution treated and is not so heavily cold worked that it would fail to meet ductility and corrosion

Y9107911

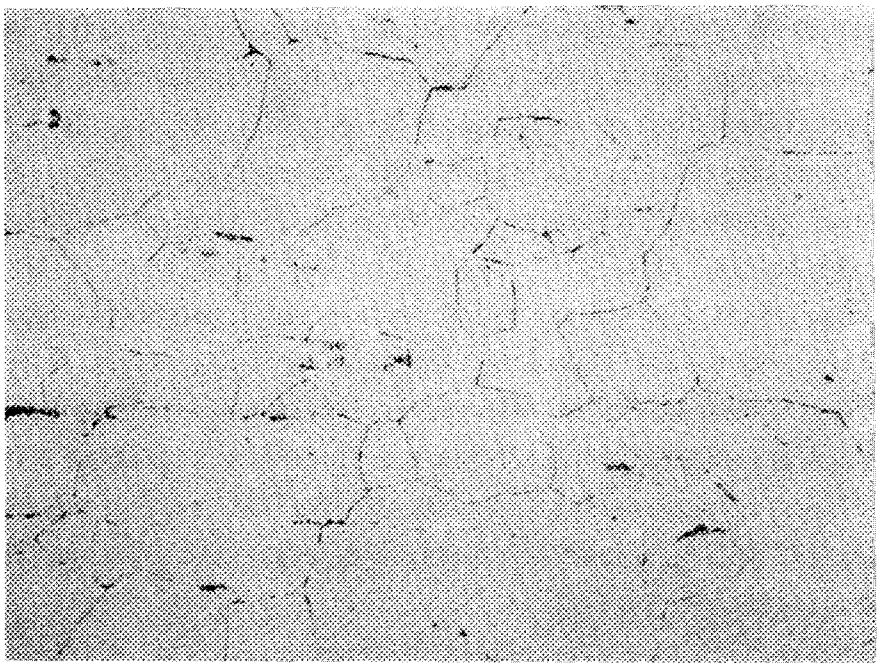

(*a*)

Y213334

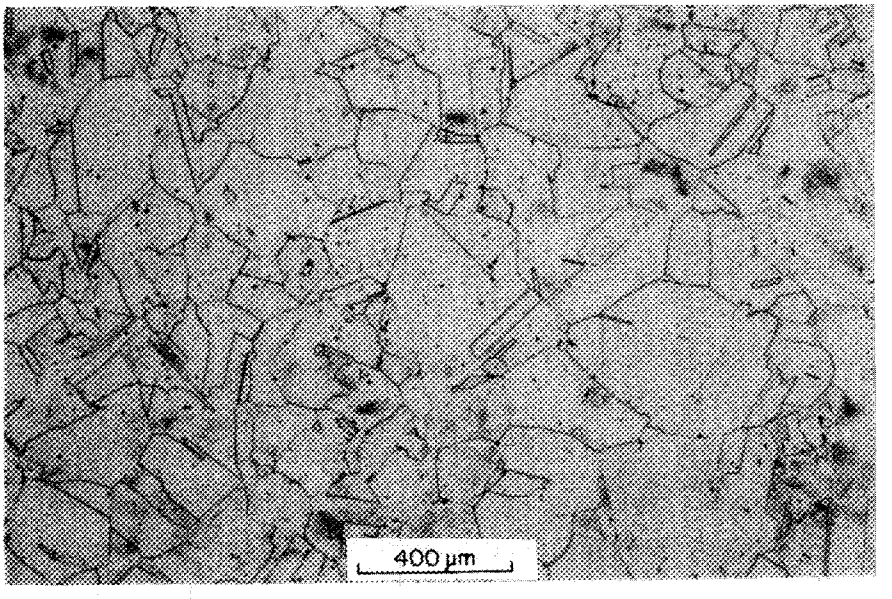

(*b*)

Fig. 7. Photomicrographs of HT-UPS tubing: (*a*) CET2 and (*b*) BWT.

requirements. In actual fact, warm work and modest amounts of cold work are often introduced as part of the surface finishing and straightening processes. It is this unspecified work, introduced at the mill, which makes it difficult to correlate composition with chemistry as might be expected when using the correlation of Irvine et al. (1969) given in Eq. (7). Because of the importance of warm or cold work to the character of the MC and MN precipitation, small variations in the fabrication history may produce large differences in the subsequent creep-rupture strength.

The NF709 and HR3C alloys do not require cold working to promote higher design allowables than conventional alloys, since they are strengthened by nitrogen. A typical yield strength for NF709 stainless steel is 340 MPa and the minimum is near 300 MPa. The HR3C alloy exhibits a typical yield strength near 360 MPa and the minimum is above 300 MPa.

Alloy 800HT has a typical yield strength near 240 MPa (INCO 1989), but the minimum strength falls near 172 MPa. It seems likely that some degree of cold work must be present to produce a yield strength above 200 MPa.

The AX series of HT-UPS alloys exhibited yield strengths around 210 MPa after annealing at 1200°C (Fig. 4), and the CET2 tubing had a yield near 290 MPa after annealing at 1125°C. The BWT7 tubing, when solution treated at 1200°C, produced a room-temperature yield strength near 240 MPa. To promote the fine MC precipitation in the HT-UPS alloys, it would be necessary to specify a minimum room-temperature yield strength in excess of 300 MPa. This would require a minimum cold working strain of 5%. Additional studies are under way on the extruded tubing to establish optimum cold-working schedules.

Providing that cold working of the products to levels of 5% strain is acceptable, it appears that Criterion II-B can be met for all near-commercial and developmental alloys.

II-C. Tubing alloys will be compatible with high-nickel, high-chromium cladding alloys.

Flately et al. (1987) produced alloy 800H tubing clad with alloy 671 by coextrusion and exposed the tubing to 34,000-h boiler service in the range of 650 to 680°C. Post-exposure testing indicated that the alloy 671 cladding was embrittled, but the alloy 800H remained ductile. Smith and Lipscomb (1987) produced alloy 800HT clad with an experimental alloy (8XA) by coextrusion and exposed the duplex tubing to an incineration environment in the temperature range of 593 to 871°C. They reported satisfactory performance.

Cladding technology for the HT-UPS alloy BWT7 tubing was developed by Topolski (1991). Here, a machined billet (133 mm in diam) was encased in a mild steel can that was subsequently filled with 50-mesh powder (either alloy 671 or 690). The can was preheated, evacuated, sealed, and extruded. The extrusion work was performed by AMAX Corporation

and the cold finishing by Babcock and Wilcox. The alloy 671 cladding extruded with no problems, but cracking occurred during the cold finishing. The alloy 690/BWT combination was successfully processed to cold-finished clad tubing and is currently undergoing evaluation (See Fig. 8).

Weld overlay was examined as a possible cladding method by LeBeau (1990). Here, a piece was sawed from the BWT billet and rolled to 13-mm plate. Alloy 690 and alloy 672 filler wire were deposited on the plate using the gas tungsten arc (GTA) process. The clad plate was then hot rolled to produce the excellent bonding shown in Fig. 9.

It appears from the information provided above that the alloys may be clad with high-nickel, high-chromium alloys, but the performance of specific claddings under the conditions imposed by advanced steam cycle operations has yet to be determined. There is reason, at this time, to believe that Criterion II-C can be met for most alloys.

II-D. The alloys will be weldable by procedures specified in the ASME BPV Code, Sect. I on Power Boilers.

The American Welding Society defines weldability as "the capacity of material to be welded under the imposed fabrication conditions into a specific suitably designed structure and to perform satisfactorily in the intended use." Welds have been produced in all of the advanced alloys, and information is provided in Table 4.

Alloy 800HT is typically welded with Inconel A, alloy 82, or alloy 117 (INCO 1989).

Takahashi et al. (1989) discussed the weldability of NF709 stainless steel. They were able to produce sound welds by the GTA process using matching filler metal. Weldment properties were similar to base metal, and the weldability was claimed to be comparable to type 347 stainless steel.

The weldability of HR3C stainless steel was reported by Yoshikawa et al. (1989). Varestraint testing revealed that the weldability was comparable to type 347 stainless steel. Partly for this reason, filler metals of differing compositions were selected for butt welding tubes. Included were alloys 625, 82, 182, and Inconel A®. Sound GTA and shielded-metal arc (SMA) welds were made in heavily restrained tubes.

A review of the welding technology for the HT-UPS alloys was undertaken by Lundin et al. (1989). A potential weldability problem was found, aggravated by the phosphorous and niobium content of some HT-UPS alloys. A number of experiments were performed at ORNL and by Lundin et al. (1989) to evaluate the weldability of the HT-UPS alloys. These experiments included, but were not limited to, Varestraint testing

YP12520

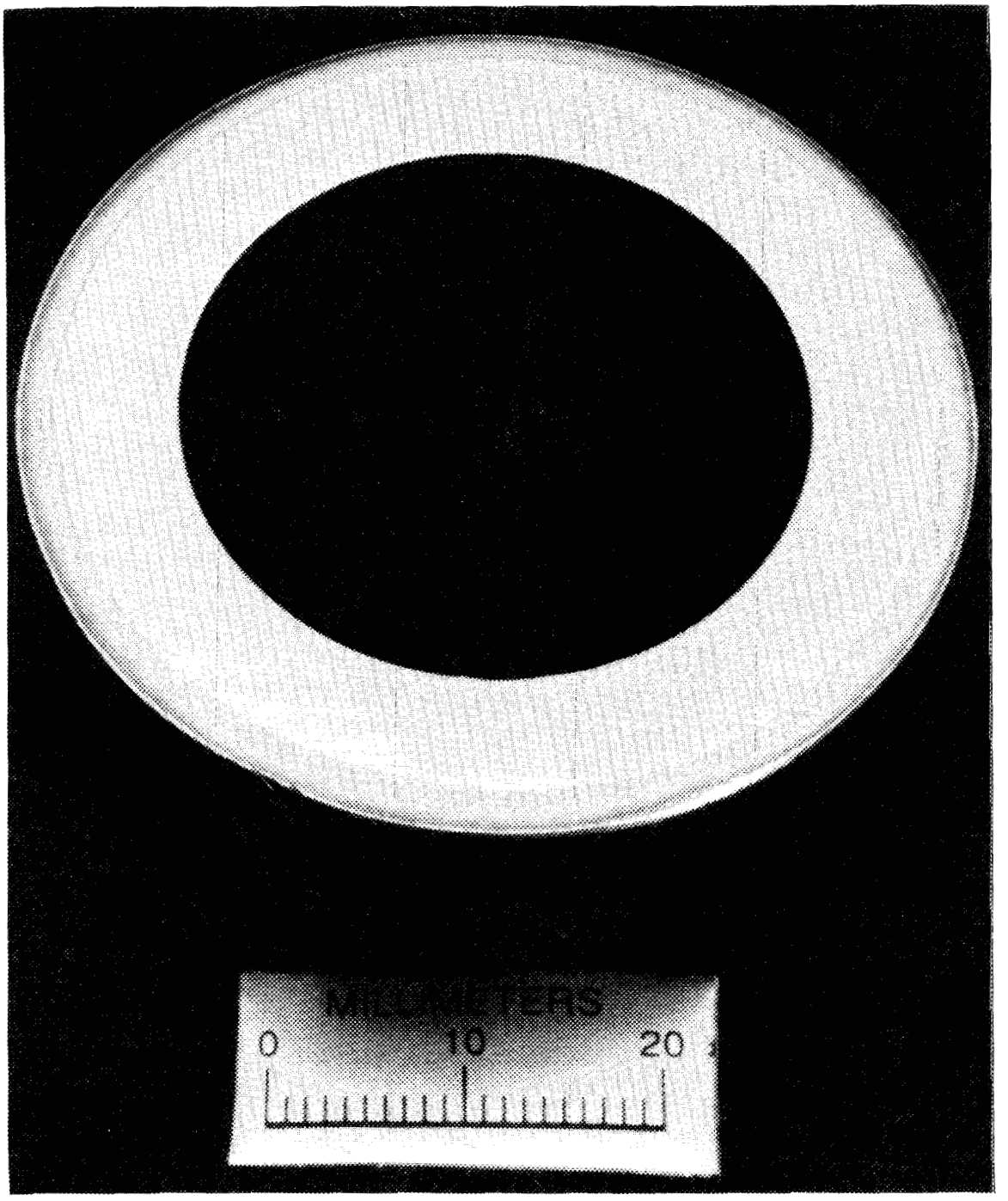

Fig. 8. Coextruded HT-UPS alloy tubing–alloy 690 on BWT.

Y213335

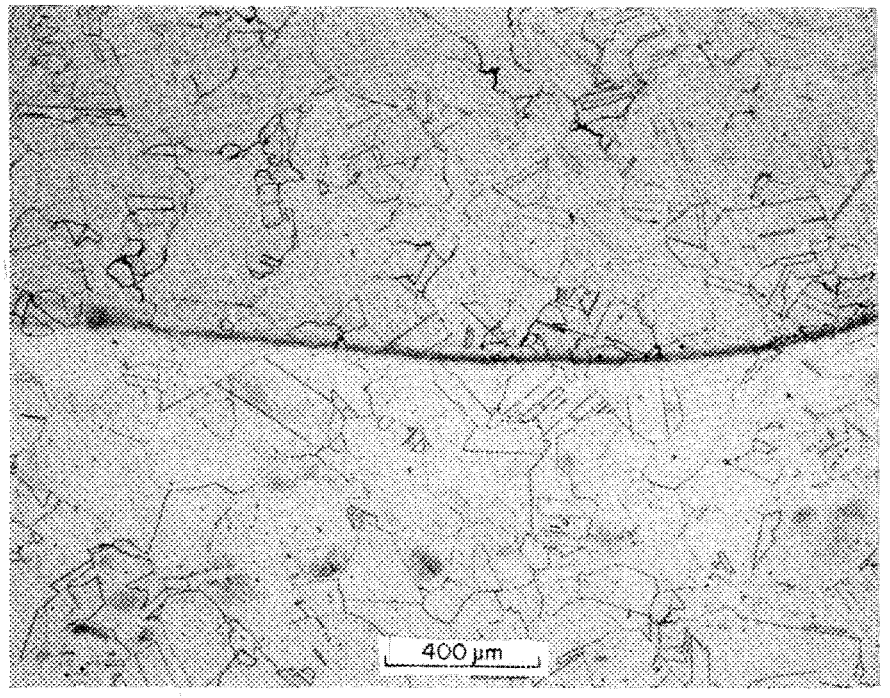

(*a*)

Y213331

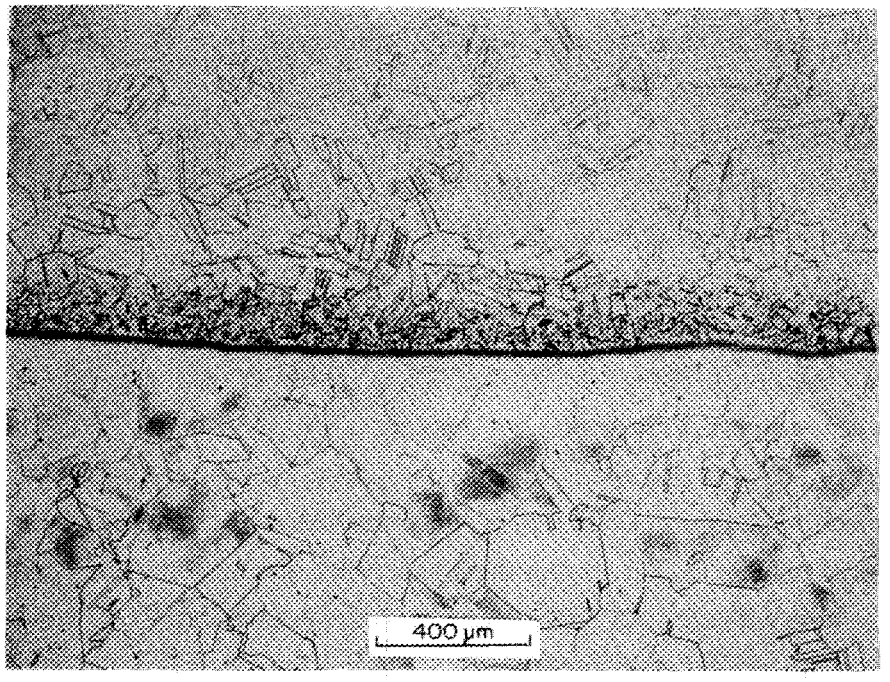

(*b*)

Fig. 9. Weld overlay and roll-clad HT-UPS plate: (*a*) alloy 690 on BWT and (*b*) alloy 672 on BWT.

Table 4. Summary of welding technology for 20/25% Cr alloys

Alloy	Filler Metal	Reference
800HT	alloy 82 alloy 182 alloy 117	INCO 1989
NF709	NF709	Takahashi et al. 1989
HR3C	alloy 82 alloy 182 alloy 625	Yoshikawa et al. 1988
AX1/AX4	17-14CuMoSS	this work
CET2	alloy 92	this work
BWT	alloy 556	this work

(Lundin et al.1985), Sigmajig testing (Goodwin 1987), and Gleeble hot ductility testing. Correlations between the various types of tests were made, and it was concluded that the alloys had a hot-cracking sensitivity equivalent to commercial, type 347 stainless steel. It was determined that the alloys could not be welded with matching filler metal.

Butt welds were produced at ORNL in several of the HT-UPS alloys. A total of six alloys were welded, plus the alloy 672 and 690 overlay cladding of the BWT7 alloy. The AX series alloys were joined with 17-14CuMo stainless steel by the SMA process. In all cases efforts were made to restrain the plates. The 13-mm plates were fillet welded to 19-mm-thick type 316 stainless steel strongbacks. After welding, side bend and metallography evaluations were performed to evaluate the extent of hot cracking. All of the AX series alloys exhibited fusion line or heat-affected-zone (HAZ) hot cracking when welded with 17-14CuMo stainless steel filler metal. The high phosphorous AX1 and AX4 heats were the worst and did not pass the visual inspection in the side bend test. Typical microstructures are shown in Fig. 10. The CET2 tubing was fillet welded to 10-mm-thick plates then clamped in the restraining rig. A butt weld was made with alloy 82. No hot cracks were found in the CET2 weld. Plates of the BWT alloy were welded with 556 filler metal. Both solution-treated and cold-rolled plates

Y208047

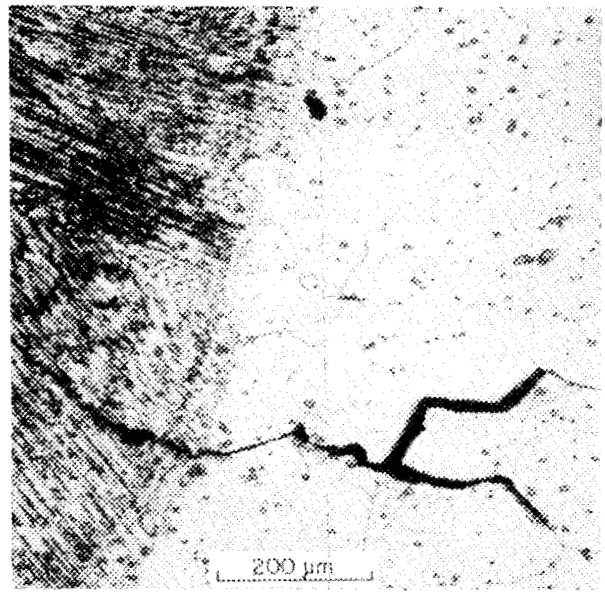

(*a*)

Y208048

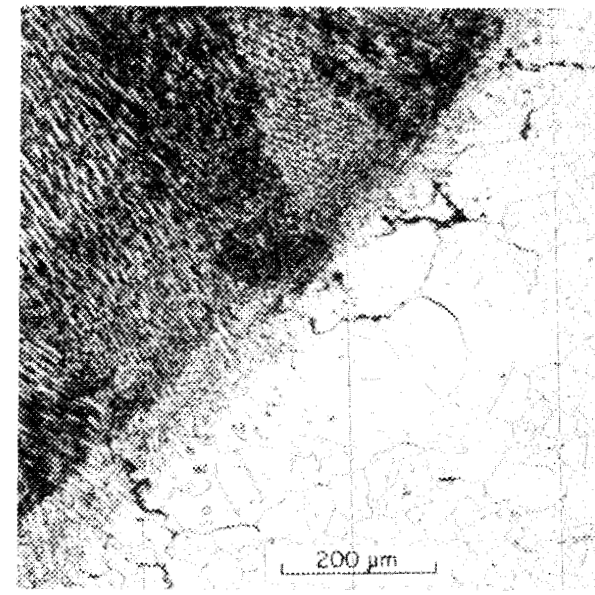

(*b*)

Y208049

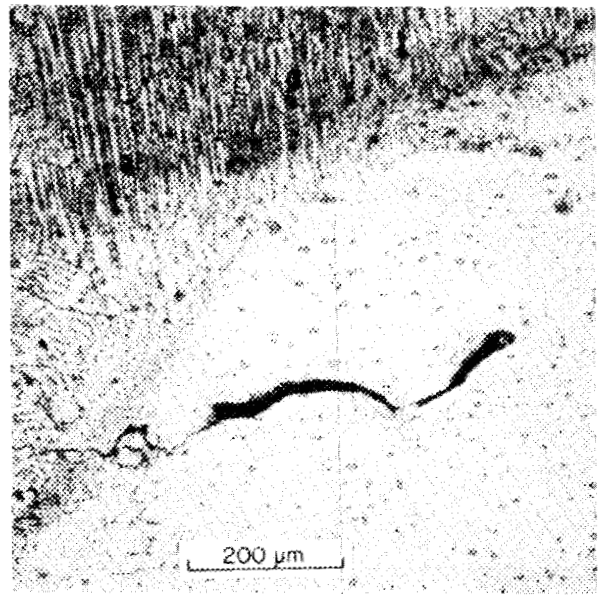

(*c*)

Y209050

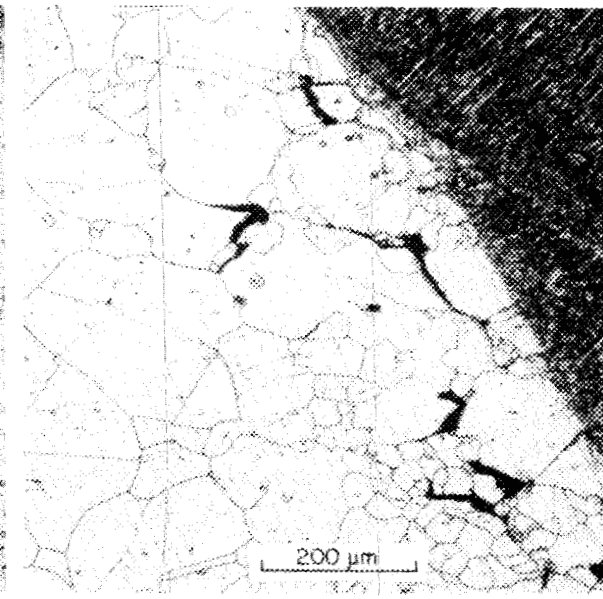

(*d*)

Fig. 10. Photomicrographs showing HAZ cracking in AX series alloys produced in welds with 17-14CuMo stainless steel filler metal: (*a*) AX1 with 0.07% P, (*b*) AX2 with 0.045% P, (*c*) AX3 with 0.03% P, and (*d*) AX4 with 0.07% P.

were welded. Although the weld appeared sound, recrystallization and grain growth were observed in the HAZ of the base metal. Typical microstructures are shown in Figs. 11 and 12. All HT-UPS alloys exhibited extensive liquation in the HAZ and, in the successful welds, it was clear that the hot cracking was avoided by virtue of the liquidity of the weld metal that was able to penetrate the open grain-boundary regions.

In summary, there are concerns about the weldability of the alloys. Extreme care will be needed in specifying the welding processes, filler metals, and process variables. Only by testing in actual boiler operating conditions can conformance to Criterion II-D be assured.

II-E. Standard practices of making tube-to-heater joints will be applicable.

The tube-to-header joint may require thick-to-thin section welds. The header could be of a different composition than the tubing, so dissimilar metal welds may be required. Several of the corrosion-resistant alloys require a special filler metal and, quite likely, such a filler metal could be used in making dissimilar metal welds. The ability to meet Criterion II-E has yet to be demonstrated.

5. MECHANICAL PROPERTIES

In specifying the alloy design criteria that address mechanical properties goals, it was intended that the strength of the tubing be sufficient to permit tubing of sizes normally used in superheaters and reheaters to operate at conditions where the fireside metal temperature could reach 700 °C and the design steam pressure reach 35 MPa (5000 psi). To use tubing of convenient diameters and wall thicknesses under these conditions, it was estimated that a design stress of 60 MPa (9 ksi) would be satisfactory. This allowable design stress intensity is approximately twice the allowable stress for any commercially available austenitic stainless steel listed in Sect. I on Power Boilers of the ASME BPV Code. One might legitimately question the need for such an ambitious target in view of the fact that the near-commercial alloys listed in Table 1 are intended for use in the advanced steam cycle and will probably function quite well at somewhat lower design stress intensities, especially in reheater tubing where the pressures are expected to be lower. The answer lies in the desire for an improved design margin. A stronger alloy provides more opportunity to optimize fabrication cost versus performance. It is assumed that a higher strength requirement will exclude the commercial alloys like type 310 stainless steel, 253MA stainless steel, and alloy 800HT, and require a careful examination of the performance of the near-commercial alloys as well. In examining

Y215475

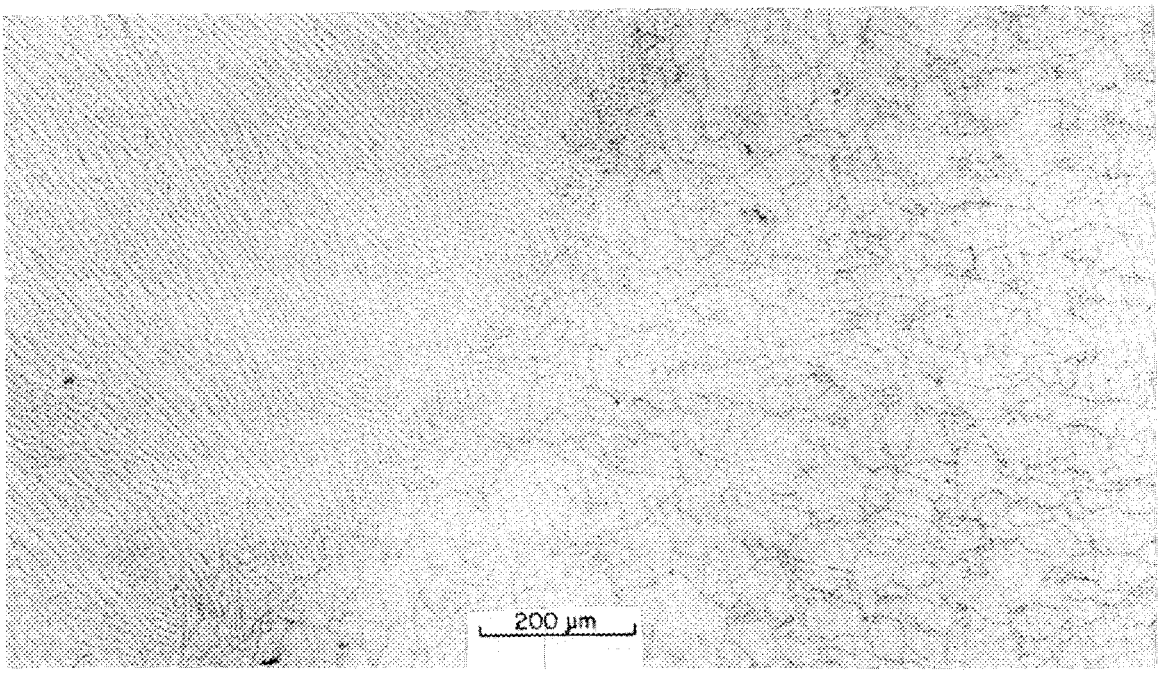

Fig. 11. Photomicrograph of weld region in cold-rolled BWT plate welded with alloy 556.

Y215471

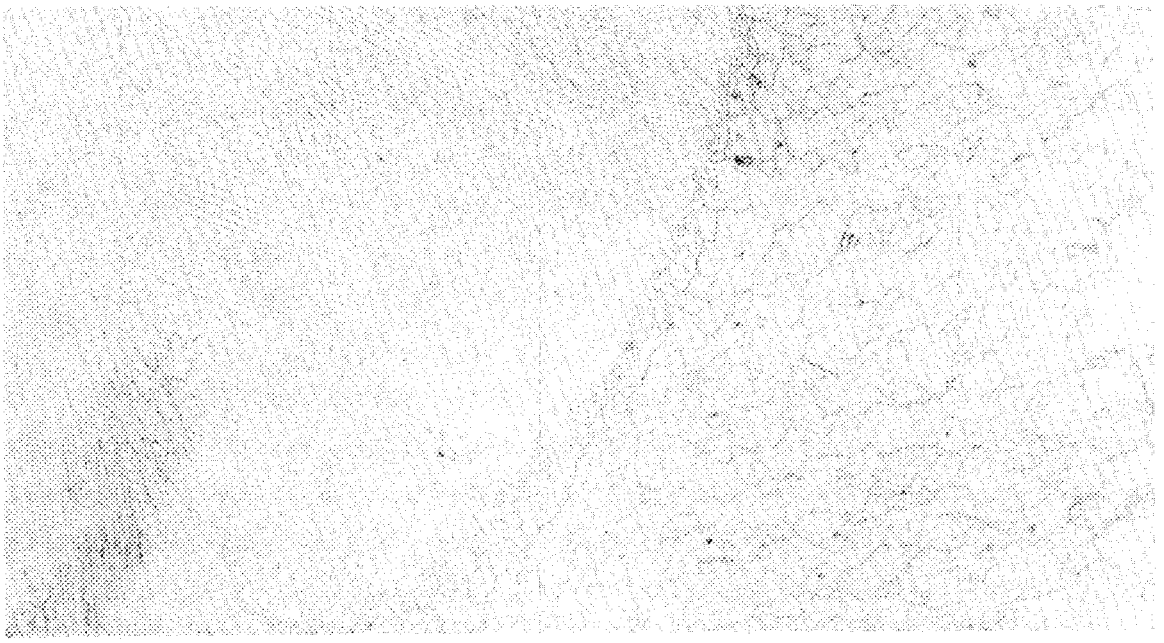

Fig. 12. Photomicrographs of weld region in annealed BWT plate welded with alloy 556.

relative performance of the alloys listed in Table 1, however, the possibility of improving any of the alloys has not been excluded, with the concomitant problems of qualifying a new grade of steel within the necessary modified specifications for chemistry or thermal-mechanical processing. Nevertheless, most of the emphasis in this section of the report will be placed on the HT-UPS alloys, and comparisons will often be made with alloy 800HT.

III-A. The design allowables will be based on the strength criteria set forth in A-150 of the ASME BPV Code, Sect. I.

Only a Code body can set design stress intensity values, and a well-defined procedure must be followed before any action can be taken by the Code to approve a new material or grade of an existing material. Of utmost importance is the need for a Code stamp on the vessel or piping system in order to meet legal requirements set by the state in which the component is to be used. Currently, there is no specific need in the United States for a high-strength boiler tubing alloy to be used in an advanced steam cycle system. Assuming that the need may exist some day, one can work toward producing materials data that could be used by the Code to establish allowable design stresses. The guidance set forth in Para. A-150 of Sect. I on Power Boilers is that the allowable design stress intensity for non-age hardenable austenitic stainless steels will be determined by:

1. 1/4 of the specified minimum tensile strength at room temperature;
2. 1/4 of the tensile strength at temperature;
3. 2/3 of the specified minimum yield strength at room temperature;
4. 2/3 of the yield strength at temperature;
5. 67% of the average stress to produce rupture at the end of 100,000 h;
6. 80% of the minimum stress to produce rupture at the end of 100,000 h; and
7. 100% of the stress to produce a creep rate of 0.01%/1,000 h.

For some austenitic alloys, such as 800HT, item (4) above has been waived, and it is permissable to use 90% of the minimum elevated temperature yield strength. Clearly, for new alloys more than one heat must be tested, and long-duration test data are needed. In addition to these requirements, evidence must be provided that the alloy does not so embrittle in long-time service that catastrophic failure could result.

Substantial data bases exist for alloys 800H, NF709, 253MA, and HR3C stainless steels. Of these, the data base for alloy 800H is well-established (Booker et al. 1978 and INCO 1986) and will be a standard against which other heats and alloys can be measured. At the

temperatures of interest, the rupture strengths of alloys 800H and 800HT were similar, and no distinction is made. The temperature ranged from 600 to 1000°C and stress-rupture times extended beyond 50,000 h at several temperatures, thus requiring a minimum of extrapolation to establish design stress allowables with a high degree of confidence.

6. TENSILE PROPERTIES

A plot of the alloy 800H yield and ultimate strength versus temperature has been provided in Fig. 13(*a*), which includes a trend line based on a simple polynomial fit through the data. The trend of the alloy 800H data may be compared with representative tensile data trends for NF709, HR3C, and 253MA stainless steels in Figs. 13(*b*) through 13(*d*), respectively. The HR3C stainless steel was the strongest, followed by NF709 stainless steel and then 253MA. The nitrogen-containing alloys were considerably stronger than the alloy 800H.

Because the quantities of the first group of HT-UPS alloys (AX) series were small and the primary application for the alloys was in the temperature range where stress-rupture strength would control the design allowables, the tensile testing of most of the developmental alloys was limited to 25 (RT) and 700°C. The exception was CET2 tubing. The yield and ultimate tensile strengths have been plotted against temperature in Fig. 14 and shown as curves. Included in Fig. 14 are the available yield and tensile strength data for other HT-UPS alloys shown as points at 25 and 700°C. Comparisons show that the 1200°C annealed HT-UPS materials were weak and the mill-annealed AX alloys (with 10% cold rolling) were strong. Comparison of the strength of the CET2 tubing with alloy 800H [Fig. 14(*a*)] indicated higher strength in the CET2 alloy. However, none of the HT-UPS alloys possessed the high ultimate strengths of the nitrogen-bearing stainless steels shown in Figs. 13(*a*) to 13 (*d*). Tensile properties for the HT-UPS alloys have been summarized in Table 5.

7. STRESS-RUPTURE

For purposes of comparison of available data on near-commercial and developmental alloys with alloy 800H on a similar time scale, the rupture strengths at 1,000 and 10,000 h were interpolated from the published data and used to calculate the Larson-Miller parameter (LMP)

$$LMP = T\,(20 + \log t_R), \tag{10}$$

ORNL-DWG 91-9609

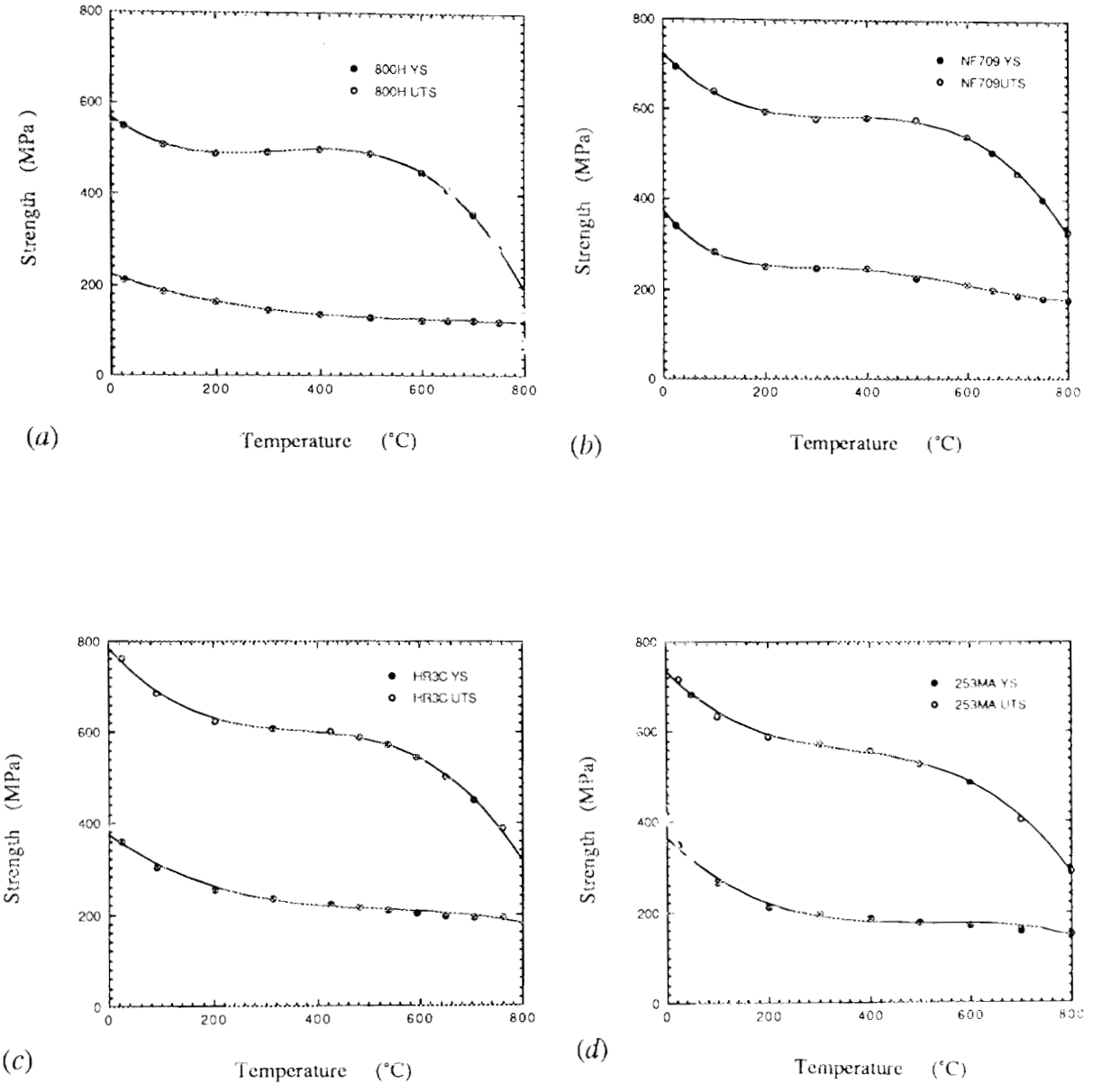

Fig. 13. Yield and tensile strengths versus temperature for several alloys: (*a*) alloy 800H, (*b*) NF709 stainless steel, (*c*) HR3C stainless steel, and (*d*) 253MA stainless steel.

ORNL-DWG 91-9610

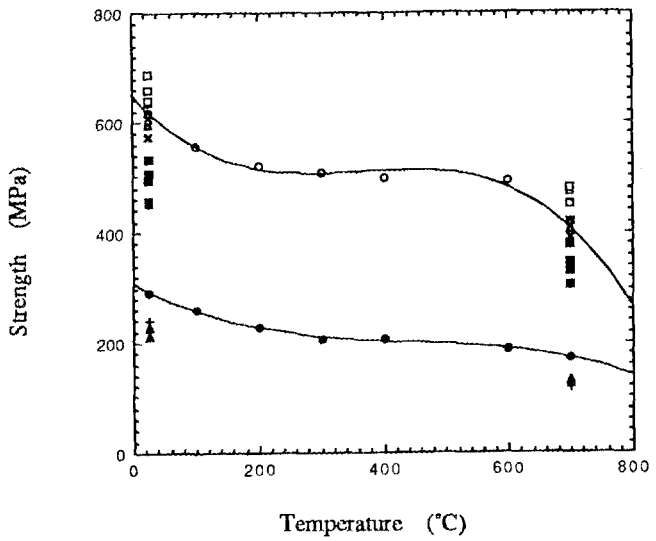

Fig. 14. Yield and tensile strengths versus temperature for HT-UPS alloys.

Table 5. Tensile data for HT-UPS alloys

Alloy	Condition	Temperature (°C)	0.2% Yield strength (MPa)	Ultimate strength (MPa)	Elongation (%)	Reduction of area (%)
800H	mill	25	180	538	54.5	61.1
AX1	mill	25	456	639	46.3	74.9
AX2	mill	25	533	690	34.6	62.4
AX2	1115 ann	25	289	643	44.1	61.3
AX2	1200 ann	25	214	598	46.5	61.3
AX3	mill	25	464	659	35.6	59.1
AX3	1115 ann	25	355	634	38.5	61.7
AX3	1200 ann	25	213	605	53.3	65.8
AX4	mill	25	507	690	39.5	64.5
AX4	1115 ann	25	368	702	39.3	56.6
AX4	1200 ann	25	230	620	54.2	58.4
AX1	mill	700	306	451	32.3	42.3
AX2	mill	700	378	418	37.2	56.0
AX3	mill	700	347	473	39.5	53.9
AX3	1200 ann	700	128	407	51.6	50.3
AX4	mill	700	330	478	36.8	56.6
CET2-01	mill	25	292	618	39.4	65.9
CET2-02	mill	100	260	556	38.4	60.7
CET2-03	mill	200	227	520	36.4	55.6
CET2-04	mill	300	205	508	38.0	51.2
CET2-05	mill	400	206	498	45.1	54.5
CET2-06	mill	500	250	517	44.8	51.0
CET2-07	mill	600	187	492	41.8	52.3
CET2-08	mill	700	171	401	3.16	35.7
BWT7-07	1200 ann	25	242	573	58.3	64.65
BWT7-11	1200 ann	700	118	390	46.8	40.54

where T is temperature in Kelvin and t_R is rupture life in hours. The resulting data are plotted in Fig. 15 where comparisons may be made to a trend line representing the log stress versus LMP for alloy 800H. The design stress intensity target identified in ORNL-6274 (60 MPa at 700°C) occurs where the LMP is 24330, and a promising alloy should exhibit an average rupture strength that exceeds the target strength by a factor of 1.5. This factor requires that the average strength at 700°C and 100,000 h should meet or exceed 90 MPa .

Alloy 800HT [Fig. 15(*a*)] is relatively weak, and a typical rupture strength for 100,000 h at 700°C is near 57 MPa.

Data for the NF709 stainless steel have been plotted in Fig. 15(*b*) and compared to the trend line for alloy 800HT. The choice of the Larson-Miller constant of 20 in Eq. 10 was reasonable, although not optimum, and the data clearly revealed excellent strength of NF709 relative to alloy 800HT. The strength at 100,000 h at 700°C has been estimated to be near 90 MPa.

The HR3C stainless steel is compared to the 800HT alloy in Fig. 15(*c*). At lower values of the LMP, the HR3C was clearly stronger than alloy 800HT but, as the value of the LMP approached the number representing 100,000 h at 700°C, the strengths converged. The estimated value for HR3C stainless steel was 60 MPa.

Type 253MA [Fig. 15(*b*)] was weak, although the LMP produced a poor fit to the data. The value based on vendor data gave a typical rupture strength for 100,000 h at 700°C near 33 MPa. There is, of course, uncertainty in the estimated strength based on the use of log stress versus LMP curves for the annealed alloys that may be attributed to the limitations in correlating the time-temperature behavior of alloys that undergo strengthening due to the precipitation of carbides during service. Actual data bases are undergoing continual evaluation by Code groups, so information provided here is, at best, only a rough estimation of the capabilities of the various alloys.

Stress rupture data for the HT-UPS alloys were highly variable, but could be separated into several groupings. The first grouping involved the "mill-annealed" AX series alloys that were solution treated at 1200°C but cold rolled to produce high-yield strengths. The second grouping consisted of the alloys solution treated at 1200°C but receiving no subsequent cold or warm work. The third grouping included those alloys that were annealed at temperatures below 1150°C. Creep and stress-rupture properties for the HT-UPS alloys have been summarized in Table 6, and the log stress versus log LMP data have been plotted in Fig. 16. The mill-annealed AX alloys [Fig. 16(*a*)] were very strong (with the exception of the mill-annealed AX4 that was brittle), and extrapolations indicated that the materials could meet the alloy strength design targets. The 1200°C annealed materials [Fig. 16(*b*)] appeared to be

Table 6. Summary of creep-rupture data on HT-UPS alloys

	TN	Spec No.	Ann	Condition	Temp (°C)	Stress (MPa)	Mcr (%/h)	t 1% (h)	t r (h)	% El	% RA	Status
1	25048	AX1-06	mill	mill	700	170	1.103-4	6500.0	8969	12.8	33.9	R
2	25384	AX1-11	1200	1200	700	170	1.00e-4	2100.0	2888	31.1	74.6	R
3	25486	AX1-12	1200	1200/2%	700	170	1.20e-4	1900.0	2572	23.7	45.6	R
4	25545	AX1-13	1200	1200/2%/Age	700	170	2.00E-4	200.0	1061	39.2	74.8	R
5												
6	25360	AX2-03	1200	1200C	700	170	1.70E-4	1800.0	2987	34.4	70.0	R
7	25412	AX2-04	1200	1200C	760	200	1.40e-2	0.6	43	32.9	68.6	R
8	25419	AX2-05	1200	1200C	760	140	6.00e-3	18.0	207	49.3	74.2	R
9	25421	AX2-07	1200	1200C	760	170	4.00e-2	6.2	88	43.0	72.7	R
10	25433	AX2-08	1200	1200C	700	200	4.60e-4	50.0	1605	33.0	72.2	R
11	25435	AX2-09	1200	1200C	700	170	1.80e-4					D
12	25440	AX2-10	1200	1200C	700	140	8.99e-5	3000.0	4831	46.6	46.7	R
13	24975	AX2-12	mill	mill	700	170	1.00e-5	6000.0	12325	15.8	64.3	R
14	25425	AX2-13	1200	1200C	760	120	2.00e-3	147.0	342	70.0	74.2	R
15	25489	AX2-15	1200	1200C	650	170	5.00e-6					37000 h
16	25487	AX2-16	1200	1200C	650	240	3.00e-5	150.0	12503	33.1	67.7	R
17	25491	AX2-17	1200	1200C	650	200	7.50e-6	10000.0	27453	28.0	72.8	R
18	25538	AX2-18	1200	1200C	760	100	6.40e-4	300.0	1072	49.5	76.7	R
19	26999	AX2-19	1200	1200/3%	760	140	5.00e-3	900.0	208	71.2	76.8	R
20	25753	AX2-20	1115	1115c	700	170	1.00e-4	60.0	1040	54.0	74.0	R
21	25739	AX2-21	1115	1115c	700	240	4.00e-3	0.4	234	30.1	73.8	R
22												
23	25681	AX3-14	mill	mill	700	240	1.20e-4	2750.0	3041	20.2	63.1	R
24	25943	AX3-15	mill	mill	760	200	5.00e-3	120.0	179	26.6	65.0	R
25	25900	AX3-16	mill	mill	730	120	1.50e-5	19700.0	21530	17.6	61.4	R
26	27166	AX3-17	mill	mill	800	140	1.40e-3	223.0	242	10.6	38.8	R
27	27412	AX3-A1	mill	700/10kh	760	200						100 h
28	27390	AX3-A2	mill	700/10kh	700	200						1200 h
29	27384	AX3-A4	mill	700/10kh	650	300			132	39.5	63.5	R
30	27381	AX3-A5	mill	700/10kh	700	170						1500 h
31	27404	AX3-A6	mill	700/10kh	700	240			298	27.0	65.3	R
32												
33	25357	AX4-01	1200	1200	700	170	7.00e-5	475.0	2232	8.5	9.2	R
34	24979	AX4-06	mill	mill	700	170	1.30e-4	1090.0	1090	3.4	2.4	R
35												
36	26058	CET2-09	mill	mill	700	200	8.70e-2		139	40.5	61.0	R
37	26084	CET2-10	mill	mill	700	197	2.50e-1		62	42.8	69.0	R
38	26089	CET2-11	mill	mill	700	170	2.50e-2	28.0	405	52.3	68.0	R
39	26111	CET2-12	mill	mill	730	170	1.60e-1	4.0	86	48.5	69.8	R
40	26120	CET2-13	mill	mill	650	275	1.80e-2	15.0	144	41.2	50.2	R
41	26119	CET2-14	mill	mill	650	200	2.80e-3	180.0	1610	31.1	70.1	R
42	26118	CET2-15	mill	mill	650	240	1.00e-2	40.0	438	43.7	67.1	R
43	26121	CET2-16	mill	mill	730	140	4.30e-2	10.0	251	47.1	67.9	R
44	26148	CET2-17	mill	mill	730	120	8.80e-3	220.0	741	50.2	73.5	R
45	26231	CET2-18	mill	mill	700	140	1.00e-2	80.0	1051	48.9	71.2	R
46	25257	CET2-19	mill	mill	760	120	7.50e-2	10.0	157	51.7	76.5	R
47	26277	CET2-20	mill	mill	700	120	1.00e-3	400.0	3497	42.7	70.8	R
48												
49	27336	BWT7-01	1200	1200	760	170	6.40e-1	1.4	14	51.8	74.0	R
50	27411	BWT7-02	1200	1200	700	170						200 h
51	27392	BWT7-04	1200	1200	765	100						1200 h
52	27339	BWT7-05	1200	1200	650	170						2000 h
53	27338	BWT7-06	1200	1200/8%	760	170	1.30e-1	5.0	34	57.4	69.5	R
54	27337	BWT7-09	1200	1200	700	170						2000 h
55	27382	BWT7-10	1200	1200	650	200						1500 h
56	27396	BWT7-13	1200	1200	600	240						500 h
57	27372	BWT7-15	1200	1200	700	140						2000 h
58	27395	BWT7-17	1200	1200	600	300						900 h

ORNL-DWG 91-9611

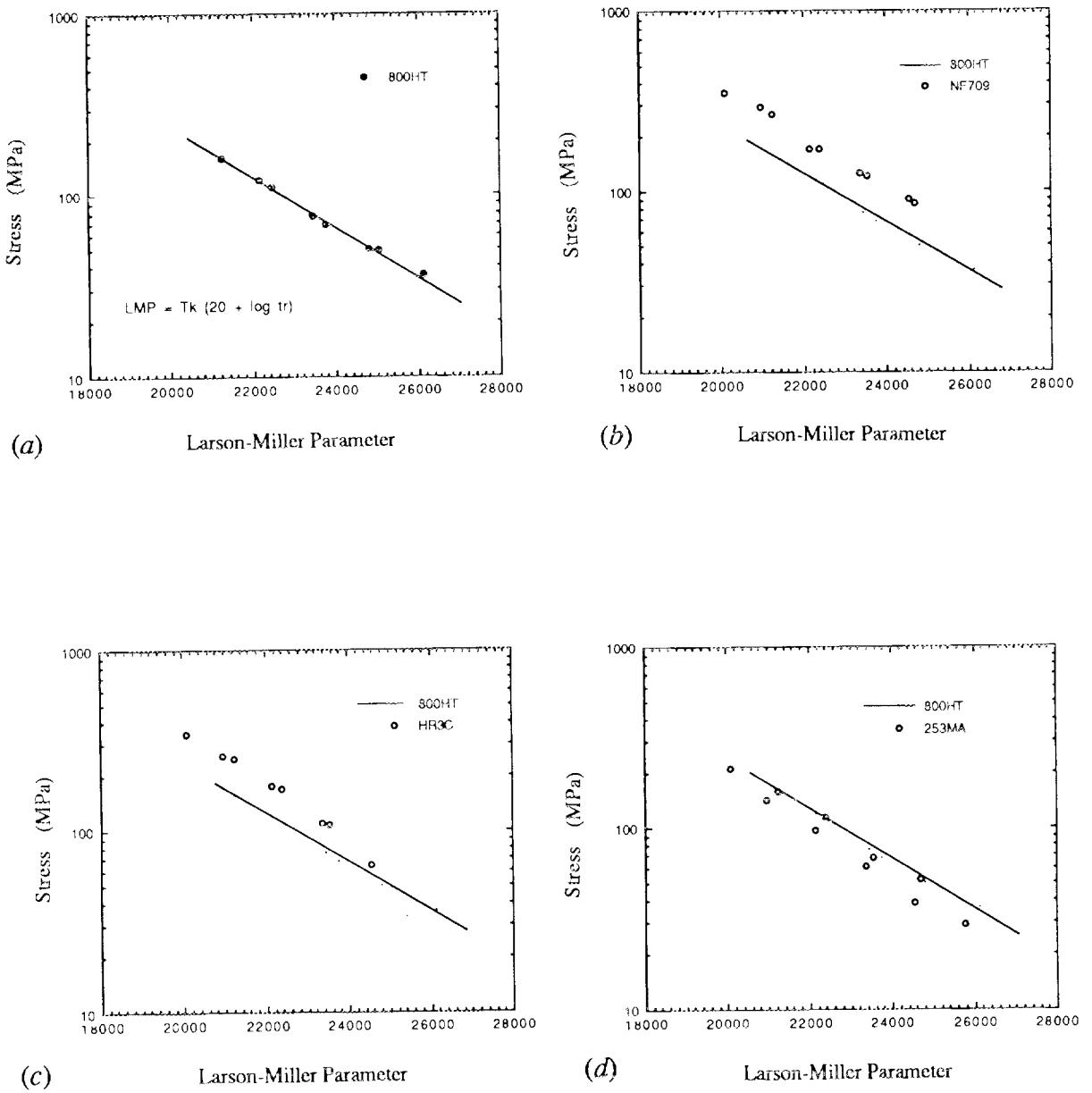

Fig. 15. Log stress versus the Larson-Miller parameter for rupture based on typical strengths at 1,000 and 10,000 h for four alloys: (*a*) alloy 800HT, (*b*) NF709 stainless steel, (*c*) HR3C stainless steel, and (*d*) 253MA stainless steel.

ORNL-DWG 91-9617

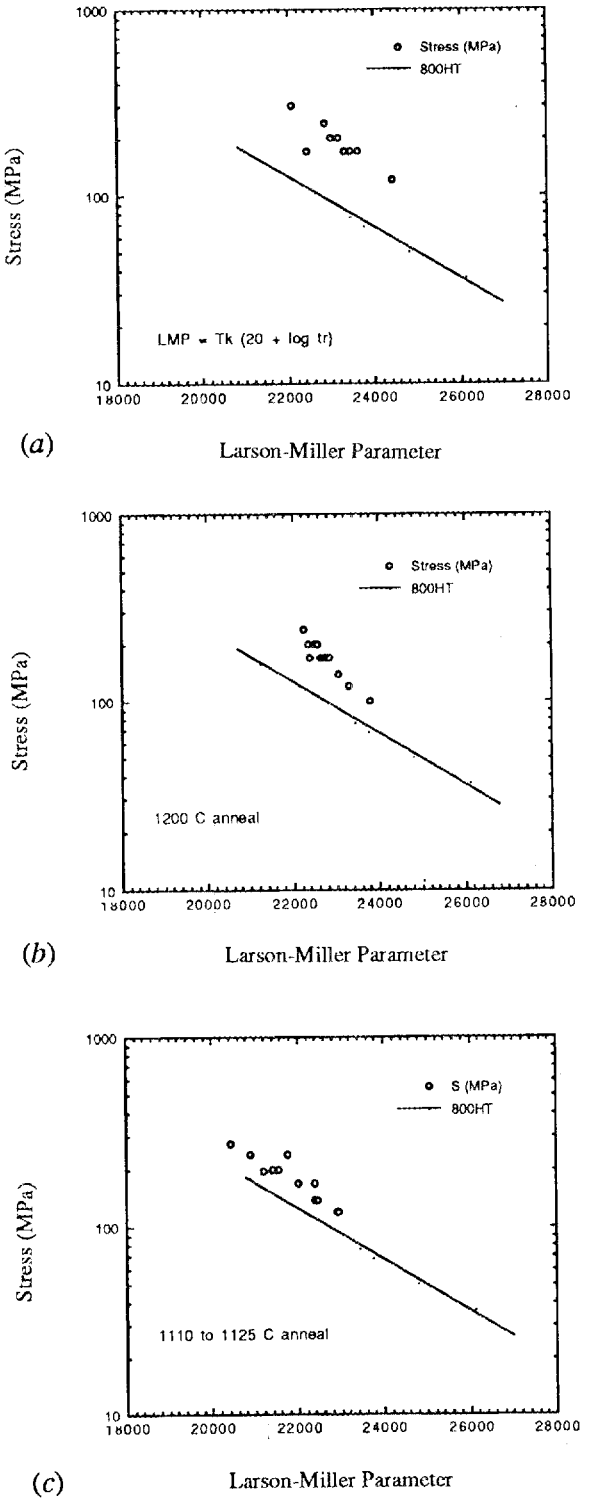

Fig. 16. Log stress versus the Larson-Miller parameter of rupture of HT-UPS alloys: (*a*) mill-annealed AX series, (*b*) 1200°C annealed material, and (*c*) lower temperature-annealed material.

strong at low values of the LMP, but the slope of the parameter curve was steep and the alloys were not much stronger than alloy 800H at the design condition. The low-temperature-annealed materials [Fig. 16(*c*)] were weak and only slightly better than alloy 800H. Testing of the BWT7 tubing is in the early stages and trends are not meaningful.

In summary, further optimization and analysis of the near-commercial and developmental alloys identified in Table 1 are required before it can be certain that the target design stress of 60 MPa at 700 °C can be achieved in fabricated boiler tubing alloys. Of the alloys investigated, NF709 stainless steel had the best chance of meeting the strength criterion. The HR3C and HT-UPS alloys show potential and may meet the criterion if the right thermal-mechanical processing scheme can been developed.

III.B. Creep-rupture ductilities will be such as to produce at least 2% circumferential strain after 100,000 h under pressurized tube rupture conditions.

Many indices have been proposed that correlate creep-rupture ductilities measured under constant-load, isothermal, uniaxial stress conditions with performance under more realistic loading conditions. Twenty-one of these indices were reviewed by Manjoine (1975) and the triaxiality factor (TF) proposed by Davis and Connelly (1959) emerged as a useful index for evaluating ductility requirements for pressurized tubing. Here, the TF is defined as the ratio of the normal stress to the shear stress on the octahedral plane, normalized to unity for simple tension

$$TF = \sqrt{2}\,(\sigma_1 + \sigma_2 + \sigma_3) / [(\sigma_1 - \sigma_2)^2 + (\sigma_2 - \sigma_3)^2 + (\sigma_3 - \sigma_1)^2]^{1/2}, \qquad (11)$$

where the principal stresses are σ_1, σ_2, and σ_3. The strain measured in the stress rupture experiment is then plotted against the TF to estimate ductility. Manjoine provided data for type 304 stainless steel, but very little information is available for the advanced alloys of interest here. Knowing the long-time ductility, an estimate may be made of the strain at rupture in a pressurized tube from the curves developed by Manjoine (1975) from type 304 stainless steel data, using the TF defined in Eq. (11) above. The ratio of ductility in a pressurized tube to the uniaxial ductility for a creep rate near 0.01%/1,000 h would be near 0.7. Assuming that the trend for elongation versus log time extrapolates to 4% in 100,000 h, the expected ductility in a pressurized tube would be around 3% ,which exceeds the 2% strain specified in the alloy design criteria.

All of the advanced alloys exhibited creep-rupture ductilities that exceed 4% in the time range where data are available. Elongation and reduction of area data for the HT-UPS alloys are plotted in Fig. 17. For the most part, excellent ductilities were observed for times to beyond 10,000 h at all temperatures.

Some concerns remain in regard to rupture ductilities under pressurized stress conditions because of the unusual failure mode exhibited by the AX series of HT-UPS alloys. As may be seen in the creep curves shown earlier (Fig. 5), the cold-rolled alloys often experienced little or no creep for long times. Over a relatively short time span, tertiary creep occurred and the specimens necked down and failed by a plastic instability mechanism. This necking and instability appeared to be brought about by recrystallization on grain boundaries and within the matrix. The MC was then dissolved into the dislocation-free recrystallized regions as shown in Fig. 18. Additional testing under variable stresses, temperatures, and multiaxial stresses are needed to establish the ductility limits of the HT-UPS alloys.

Currently, the existing data suggest that the advanced alloys have adequate ductility to meet Criterion III-B.

<u>III-C. Over-temperature excursions of 50 °C for up to 1% of life will not degrade long-time strength by more than 10%</u>.

High-temperature heat recovery systems generally experience over-temperature transients with various degrees of severity. Very little testing has been performed to assess the ability of alloys to resist such transients without undergoing damage. One significant symposium was held by ASTM (1954) that collected work on cyclic heating and stressing of materials, and the trends revealed in the papers on austenitic stainless steels indicated that the linear damage summation proposed by Robinson (1952) was satisfactory in correlating data. Here, the creep damage fraction, d_{ci}, during any transient to temperature T_i is calculated by

$$d_{ci} = \delta t_i / t_{ri}, \tag{12}$$

where Σt_i is the time at T_i and t_{ri} is the time to rupture at that temperature and stress. When the sum of all damage fractions reaches unity, failure occurs

$$\Sigma\ d_{ci} = 1.0\ . \tag{13}$$

ORNL-DWG 91-9613

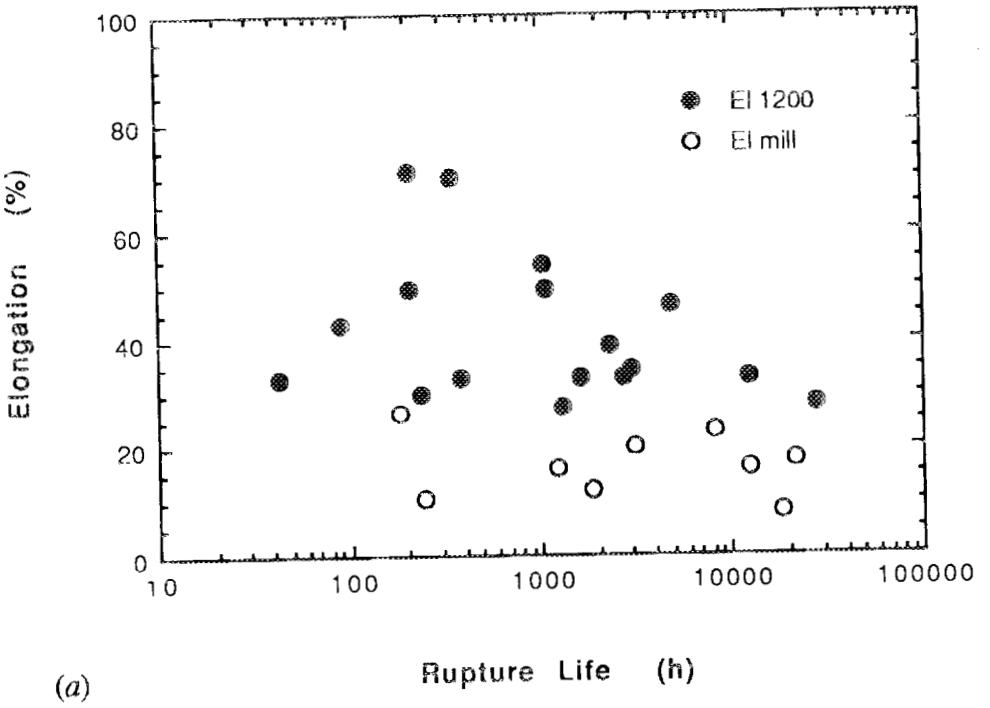

(*a*)

ORNL-DWG 91-9614

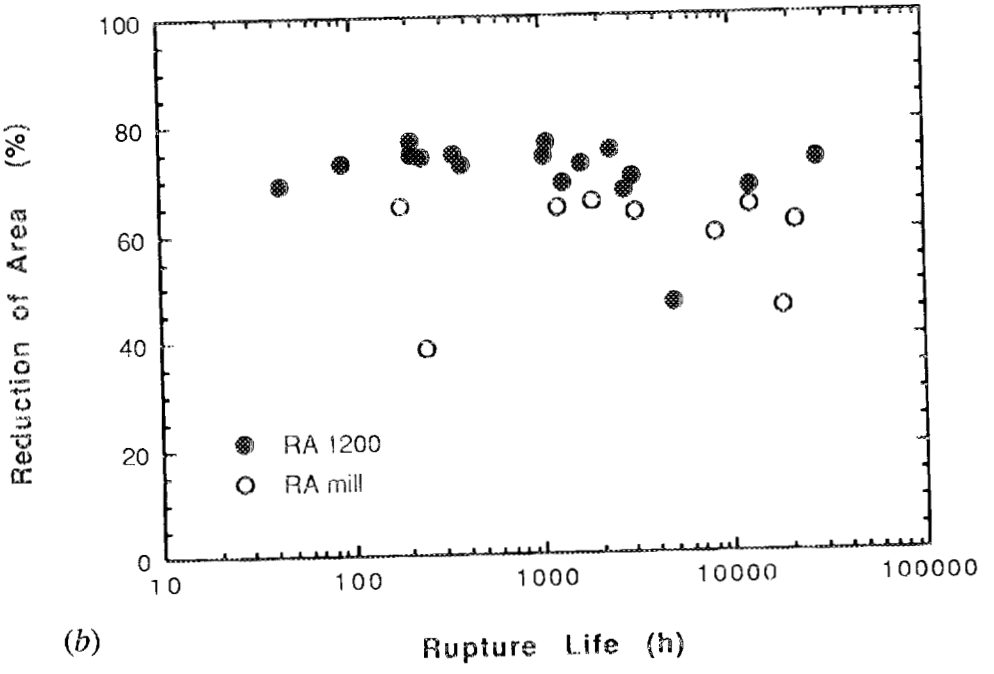

(*b*)

Fig. 17. Ductility versus rupture life for HT-UPS alloys: (*a*) elongation and (*b*) reduction of area.

YE-14155

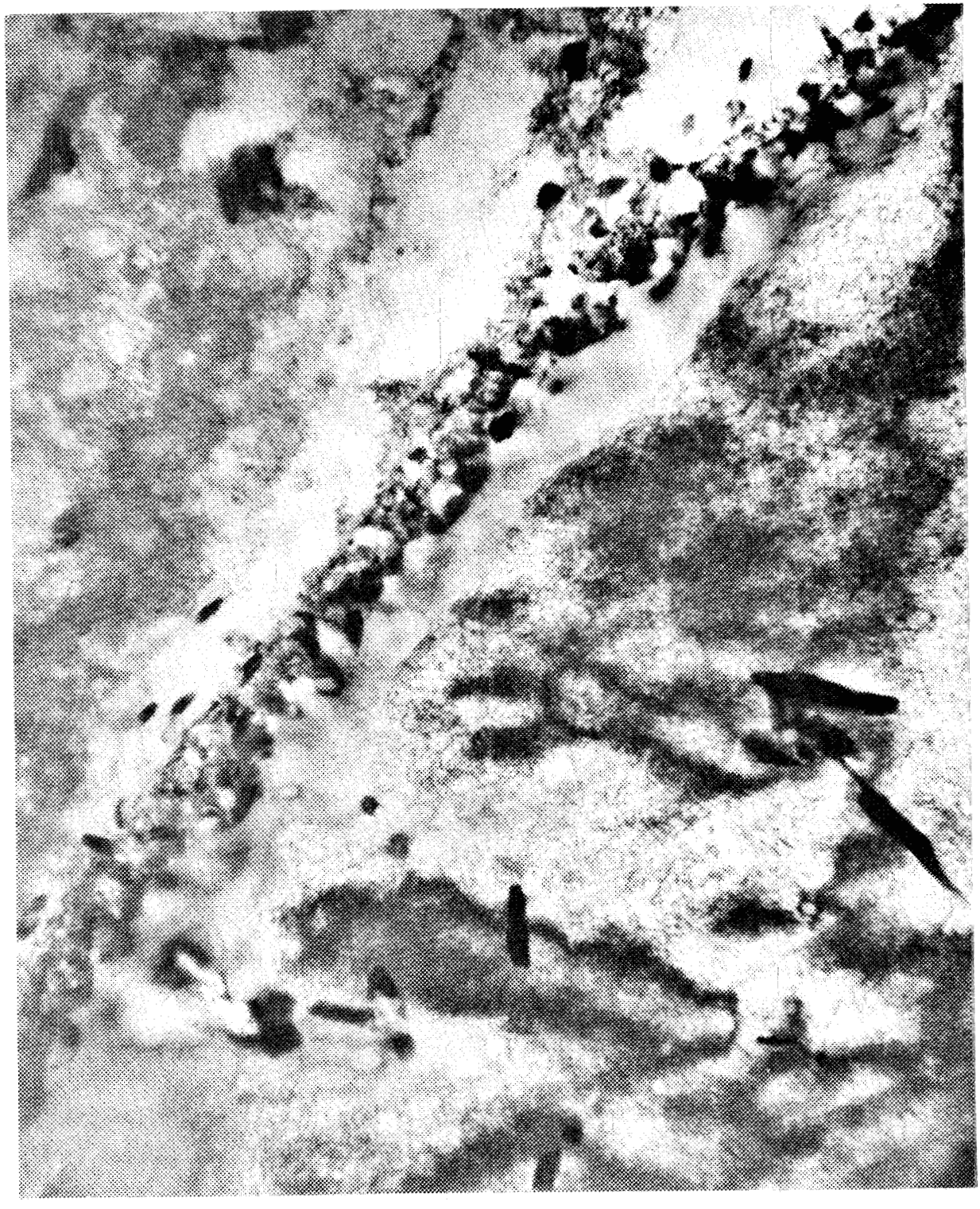

Fig. 18. TEM of HT-UPS alloy AX2 showing regions of recovery/recrystallization after 12,500 h at 700°C and 170 MPa.

Criterion III-C assumes the validity of linear damage but allows a significant extent of damage due to transients to be accumulated. Examining the general trend of the LMP curves plotted earlier and taking 90% of the stress for any LMP value, the reduced LMP value and the original LMP value for that stress may be used to estimate the percent of life corresponding to a 10% loss of strength. For the HT-UPS alloys, this procedure estimated an allowable 50% loss in life at stresses in the range of the LMP curve. In other words, if the damage fraction summation for tests involving temperature changes exceeds 0.5, Criterion III-C can be satisfied for a given alloy.

No information is currently available for the advanced alloys. A few tests on the HT-UPS alloys to examine damage under temperature change conditions are currently in progress, but data are incomplete at this time.

III-D. Stress-temperature cycling will not degrade the long-time strength by more than 10%.

Reflecting the concerns in the boiler industry about material degradation under cyclic loads, Criterion III-D addresses the need for an understanding of damage accumulation under both temperature and load cycling. Fatigue and creep-fatigue interaction phenomena are known to produce significant damage in austenitic stainless steels at high temperatures, and much is being done to reduce the likelihood of cycle-induced failures. Currently, the rules used most often for evaluating damage under combined stress- (or strain-) temperature cycling are those in the high-temperature extension of the ASME BVP, Sect. VIII, namely Code Case N-47. Here, continuous cycling design fatigue curves were constructed from uniaxial, strain-range-controlled, low-cycle fatigue (LCF) tests. It was then recommended that the fatigue damage for any arbitrary cycling histogram be calculated from Miner's rule. Various types of creep damage are then introduced in the cycle and the creep damage fraction calculated from Robinson's rule (1952). The fatigue damage fraction, d_{fi}, for any cycle at strain range, $\Delta\varepsilon_i$, is given by

$$d_{fi} = 1/N_{fi} , \tag{14}$$

where N_{fi} is the number of cycles to failure at $\Delta\varepsilon_i$. Again, damage is summed over all cycles but, for creep fatigue interactions, the creep damage and fatigue damage fractions are again summed and the total damage, D, restricted to a number equal to or less than 1. Thus

$$D = \sum d_{ci} + \sum d_{fi}. \tag{15}$$

For austenitic stainless steels, D is sometimes chosen to be 0.3.

Of the alloys identified in Table 1, only alloy 800H has a sufficient data base to estimate the D value by the analysis method developed for Code Case N-47, and the value of D was specified as unity. Some progress has been made in understanding creep fatigue damage in 253MA by Nilsson (1988) and in type 310 stainless steel by Kanazawa et. al. (1988). Nilsson found that 253MA was more sensitive to creep damage in hold-time fatigue than type 316 stainless steel. Indications were that D would be 0.3 or less. Kanazawa studied strain- rate effects at a number of temperatures and found significant losses in fatigue life at low strain rates when temperatures were in the range of 600 to 700°C. Doi et al. (1986) found that the low-cycle fatigue resistance of Hitachi-modified 800H was slightly better than alloy 800H.

Further studies on cyclic operation and the way in which damage is summed are needed to determine if Criterion III-D can be met for the high-chromium alloys.

III-E. Notched-to-smooth-bar, creep-rupture strength ratios will exceed unity at temperatures in the range of 600 to 760 °C.

No data are available on the notched stress-rupture behavior of the advanced alloys.

III-F. Charpy V impact energy at room temperature will exceed 20 J at the end of life.

Yukawa (1991) reviewed research on the influence of aging on the impact energy and fracture toughness of austenitic alloys. The impact energy (Charpy V, Charpy keyhole, or Izod) of most alloys diminished as a result of long-time aging.

Alloy 800H appeared to be a good performer. INCO reported the impact strength of 20% cold-rolled alloy 800HT after exposures to 12,000 h at 540 and 650°C. The Charpy V impact values exceeded 80 J.

Data reported for HR3C stainless steel indicated satisfactory Charpy V impact values (Yoshikawa et al. 1988). Energies exceeded 40 J after 10,000-h exposures at temperatures in the range of 600 to 800°C.

NF709 stainless steel exhibited significant losses in impact energy as a result of aging at 700°C, but values stabilized above 30 J after 10,000 h. Little is known about the aging characteristics of the HT-UPS alloys.

In summary, all of the alloys listed in Table 1 will lose toughness as a result of exposure to high-temperature service. Further studies of loss of toughness in a service environment are needed.

III-G. Impact properties of weld metal will meet the requirements of the ASME BPV Code.

Austenitic alloy weldments that contain significant amounts of ferrite could suffer embrittlement if the ferrite were to transform to sigma or α' during service. The advanced alloys are not expected to contain much ferrite in welds. Nevertheless, sigma, Laves phase, and carbides in welds could produce embrittlement. No information has been produced on the aging embrittlement of weld filler metals.

In summary, more information is needed on the toughness of aged filler metal for all alloys listed in Table 1. In particular, the nickel-base filler metals and alloy 556 filler metal should be investigated to determine their tendency toward embrittlement. Work on alloy 556 by McCoy and King (1985) indicated significant embrittlement of alloy 556 welds.

III-H. The creep-rupture strength of weldments will exceed 90% of the base metal strength.

Data for the strength of weldments have been reported for some of the advanced alloys. Generally, the criterion of 90% of the base metal strength has been met.

For alloy 800HT weldments, the alloy 82 filler metal was reported to be stronger in stress rupture than the base metal (INCO 1989).

For HR3C stainless steel, the weldments produced with alloy 82 filler metal ruptured at times that fell into the scatterband for base metal (Yoshikawa et al. 1988).

For NF709 stainless steel, the weldments produced with matching filler metal were equivalent or stronger in stress rupture than base metal (Takahashi et al. 1989).

As discussed in Sect. 4 of this report, the results of the tests for weldability of the HT-UPS alloys indicated that their high nickel equivalent would preclude autogenous welding, and the alternate filler metals and processes are identified in Table 4. These included alloy 82 (a nickel-base alloy), 17-14CuMo stainless steel, and alloy 556 (a Fe-Ni-Cr-Co alloy). Screening tests of weldment strength and ductility consisted of tensile tests on transverse weldments at 25 and 700°C, creep tests on transverse weldments at 700°C and 170 MPa, and a few creep tests at temperature in the range of 600 to 800 °C to examine time-temperature-stress effects. Data on weldments have been summarized in Table 7 for tensile behavior and Table 8 for stress-rupture behavior. Results are preliminary and do not reflect the optimum selection of welding combinations.

In summary, more testing of full-scale weldments and pressurized tubes with weldments is needed to assure that dissimilar weld failures of the type reviewed by

Table 7. Tensile data for HT-UPS alloy weldments

Specimen	Alloy	Filler	Temperature (°C)	Yield strength (MPa)	Tensile strength (MPa)	Ultimate elongation (%)	Reduction of area (%)	Failure location
AXW1-01	AX1	17-14CuMoSS	25	461	603	09.0	18.3	fusion line
AXW1-02	AX1	17-14CuMoSS	700	316	414	17.5	17.6	fusion line
AXW2-01	AX2	17-14CuMoSS	25	515	684	19.6	47.6	weld
AXW2-02	AX2	17-14CuMoSS	700	345	414	13.4	39.2	weld
AXW3-01	AX3	17-14CuMoSS	25	494	639	11.9	28.1	weld
AXW3-02	AX3	17-14CuMoSS	700	329	428	20.1	21.1	fusion line
AXW4-01	AX4	17-14CuMoSS	25	474	510	01.2	02.5	fusion line
AXW4-02	AX4	17-14CuMoSS	700	264	264	00.8	00.4	fusion line
SET1-01	BWT	556	25	425	664	25.8	61.9	HAZ
SET1-02	BWT	556	700	284	403	25.3	66.4	base
SET1-04	BWT	556	760	281	330	29.6	73.0	base
SET1-05	BWT	556	600	289	493	02.4	54.8	weld
SET2-01	BWT	556	25	456	698	25.1	62.3	base
SET2-02	BWT	556	700	286	446	22.5	47.0	HAZ

Table 8. Stress rupture of weldments in HT-UPS alloys

Specimen	Alloy	Filler	Temperature (°C)	Stress (MPa)	Life (h)	Reduction of area (%)	Failure location
AXW1-03	AX1	17-14CuMoSS	700	170	3222	05.60	weld
AXW2-03	AX1	17-14CuMoSS	700	170	2858	00.60	weld
AXW3-03	AX2	17-14CuM0SS	700	170	2899	01.60	weld
AXW4-04	AX2	17-14CuMoSS	700	170	172	00.10	fusion line
SET1-07	BWT	556	760	200	3.7	76.60	base
SET1-08	BWT	556	760	170	11.7	81.00	base
SET1-09	BWT	556	760	140	75	75.10	base

Roberts et. al. (1985) would not occur. Work on weldments in HR3C and NF709 stainless steels and the HT-UPS alloys would be of value.

8. FIRESIDE CORROSION

Fireside corrosion is probably the most severe problem to be addressed in the selection of materials for heat recovery in an advanced-steam-cycle, pulverized-coal-fired boiler. Corrosion is largely due to the formation of liquid trisulfate deposits on the tubing that suppress the formation of protective oxides. In applications where the coal may have lower alkali or sulfur content, it is possible that corrosion would not be so limiting, and the alloys with at least 20% chromium could be used without protection. In specifying criteria for fireside corrosion, it was assumed that a coal such as Illinois No. 6 would be used. The corrodants produced by the combustion of this material are severe. The subject has been considered in the early work of Clark et al. (1960) and much has been examined in the ensuing 30 years. Current studies are underway by Nakabayashi et al. (1986), Wolowodiuk et al. (1989), and Plumley and Rozniak (1989), to name a few. Alloys include several of those listed in Table 1, and these are being tested both in the laboratory and in probes in boilers. Higher chromium, aluminum-bearing, and nickel-base alloys are being evaluated. A full interpretive report has been written by Van Weele and Blough (1990) that addresses the problems. Alloys listed in Table 1, which are being investigated by Blough as part of this work, include HR3C stainless steel, alloy 800H, and the HT-UPS alloys. Claddings for these alloys include alloys 671, 690, and 692. Some data are available at this time, so the criteria specified in ORNL-6274 will be covered briefly.

IV-A. Alloys will be amenable to cladding.

It has been shown in earlier sections of this report that the advanced alloys can be clad with a variety of corrosion-resistant alloys. The long-time performance of some claddings has been demonstrated in boilers that operate at steam temperatures as high as 570°C by Flately et al. (1987). Testing of cladding alloys under highly corrosive conditions has been undertaken by Blough and Van Weele (1991). For the most part, the corrosion rate diminishes with increasing chromium content. The trends are shown in Fig. 19 for some of the alloys of interest.

IV-B. Corrosion in beneficiated coal will not exceed 10% of the wall thickness during the design lifetime.

Typically, tube thinning in the Eddystone Unit 1 plant, which uses a coal with a relatively low ash content, reached 30% of the wall thickness. The results of recent probe testing in the Eddystone Unit 1 boiler were reported by Plumley and Rozniak (1989). They exposed 21 alloys for times reaching 16,000 h to corrosion from the combustion products of the relatively clean coal (6 to 7% ash and <2.5% $Na_2O + K_2O$ in the ash). The alloys containing 20% or more chromium exhibited satisfactory performance. These included alloy 800H and HR3C stainless steel. Models are now under development by Blough (1990) that will use laboratory data, probe data, and power plant experience to predict performance of alloys as a function of time, temperature, and coal chemistry.

In summary, much has yet to be accomplished in the area of addressing the fireside corrosion problems, especially with respect to the HT-UPS alloys. Probe testing in boilers would be of considerable value.

9. STEAMSIDE CORROSION

Because of concern about exfoliation of oxides that form on the steamside of the tubing and the possible damage that particulates could inflict on the turbine at the pressures and temperatures of the advanced steam cycle (Rehn 1981), a relatively stringent requirement was placed on the steamside corrosion resistance. The criterion was that the the corrosion resistance be equivalent to alloy 800. Evidence to date for Japanese experience with alloys containing at least 20% chromium indicates that steamside corrosion should not be a problem. Cold working is known to improve oxidation resistance of the lean tainless steels and could be of benefit in the higher chromium alloys as well.

ORNL-DWG 91-9615

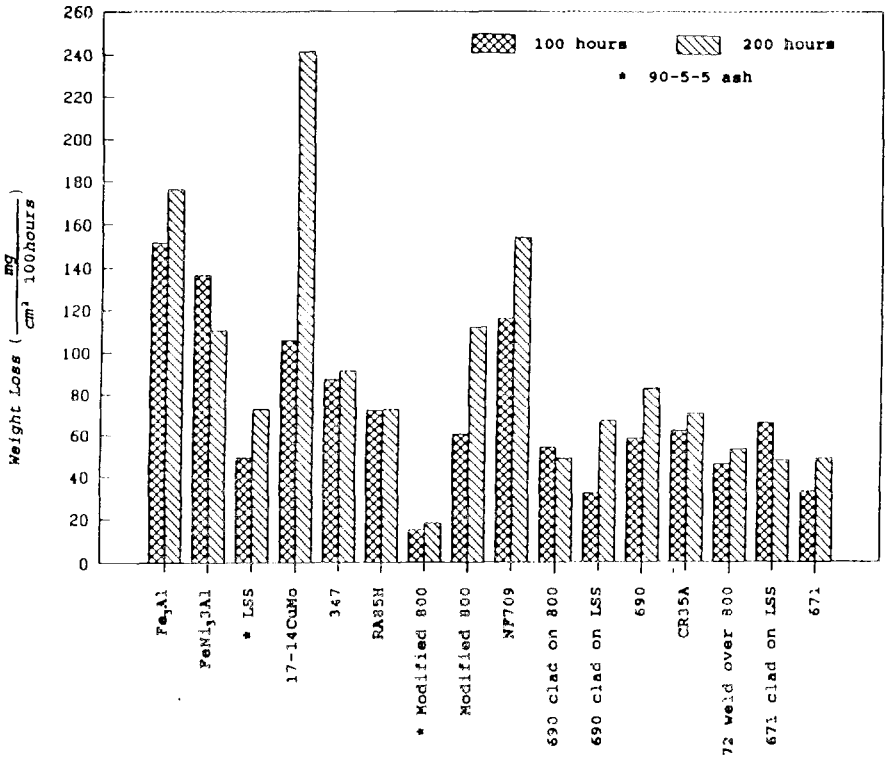

Fig. 19. Performance of candidate tubing alloys tested by Van Weele and Blough under coal ash corrosion conditions.

There may be a problem with the molybdenum- and vanadium-bearing alloys in regard to oxidation resistance at temperatures above 700°C. Solution treating in air at 1100°C has produced severe oxidation of the HT-UPS alloys as observed by Topolski (1991), and cyclic oxidation studies by INCO revealed excessive spallation (Smith 1991). Work is currently under way to introduce minor compositional changes to the HT-UPS alloys to improve the adherence of natural oxides.

10. CONCLUSIONS

1. Iron-nickel alloys containing 20% or more chromium and strengthened by MC-forming elements can be processed to produce microstructures that are stable for times exceeding 35,000 h at 700°C. The embrittling influence of intermetallic phases can be minimized by reducing the content of elements that promote sigma and Laves phase or increasing nitrogen.

2. High-strength, high quality superheater tubing can be readily fabricated from alloys resistant to steamside corrosion. For optimum properties, the HT-UPS alloy tubing should be solution treated at a temperature above 1150°C and subjected to small amounts of cold or warm work to promote the precipitation of fine MC carbides.
3. To minimize weldability problems, the HT-UPS alloys should have low phosphorous, sulfur, and other residual elements. Alloys with high nickel equivalencies, such as the HT-UPS alloys, are subject to hot cracking and require special filler metals for joining.
4. With optimized heat treatment, it should be possible to produce superheater tubing that will achieve a design stress close to 60 MPa at 700°C. Commercial and near-commercial lean stainless steels that are close to meeting the strength requirements include HR3C and NF709.
5. The practicality of protecting 20 to 30% chromium-bearing alloys from corrosion in high-ash-content coal by higher chromium alloy cladding seems likely.
7. The HT-UPS alloys possess the best strength and ductility, but techniques to produce clad tubing with controlled cold or warm work must be demonstrated.

11. ACKNOWLEDGMENTS

This activity was initiated under the guidance of R. R. Judkins, N. C. Cole of the Fossil Energy/AR&TD Materials Program, and E. E. Hoffman of DOE-OR. G. M . Goodwin participated in the development of welding procedures, Sigmajig testing, and the selection of the CRE 16-8-2 filler metal for the HT-UPS alloys. T. K. Roche reviewed the report for technical content. The metallography was performed by S. Eatherly. The report was edited by K. Spence and final manuscript prepared by M. R. Upton.

12. REFERENCES

American Society for Testing and Materials 1954, *Symposium on Effect of Cyclic Heating and Stressing on Metals at Elevated Temperatures,* ASTM STP 165, Philadelphia.

Blough, J. F. 1990. "Fireside Corrosion Testing of Candidate Superheater Tube Alloys, Coating, and Cladding," pp. 251-52 in *Fossil Energy Advanced Research and Technology Development Materials Program Semiannual Progress Report for Period Ending September 30, 1989,* ORNL/FMP-89/2, Martin Marietta Energy Systems, Inc., Oak Ridge Natl. Lab .

Blough, J. F., and Van Weele, S. 1991. "Fireside Corrosion Testing of Candidate Superheater Tube Alloys, Coating, and Cladding," pp. 211-19 in *Fossil Energy Advanced Research and Technology Development Materials Program Semiannual Progress Report for Period Ending September 30, 1990*, ORNL/FMP-90/2, Martin Marietta Energy Systems, Inc., Oak Ridge Natl. Lab.

Booker, M. K., Baylor, V. B., and Booker, B. L. P. 1978, *Survey of Available Creep and Tensile Data for Alloy 800H*, ORNL/TM-6027, Union Carbide Corp. Nuclear Div., Oak Ridge Natl. Lab.

Chapman, E. C., and Lorentz, R. E. Jr., 1960. "The Selection of Materials and Fabricating Techniques for the Eddystone Boiler and Sulzer Control Valves," pp. 275-85 in *J. Eng. Power*, American Society of Mechanical Engineers, New York.

Clark, C. L., et al. 1960. "Metallurgical Evaluation of Superheater-Tube Alloys after Six-Months' Exposure at Temperatures of 1100 to 1500 F," pp. 35-67 in *J. Eng. Power*, American Society of Mechanical Engineers, New York.

Davis, E. A., and Connelly, F. M. 1959. "Stress Distributions and Plastic Deformation in Rotating Cylinders of Strain Hardening Materials," *J. App. Mech.* **81**, 25-30.

DeLong, W. T. 1974. "Ferrite in Austenitic Stainless Steel Weld Metal," *Weld. J.*, 273-s-286-s.

Doi, H., et al. 1986. "Effects of Nb and Mo on Creep Rupture Strength of 23Cr-34Ni Iron Based Alloy," pp. 227-32 in *Proceedings, International Conference on Creep*, Japan Society of Mechanical Engineers, Tokyo.

Domian, H. A., and LeBeau, S. E. 1989. *Literature Review of Workability and Phase Stability Relative to Advanced Austenitic Alloys in Steam Service*, ORNL/SUB/88-SB775/01, Martin Marietta Energy Systems, Inc., Oak Ridge Natl. Lab.

Ellis, F. V., et al. 1988. *Composition and Sigma Phase Determination in Eddystone No. 1 Main Steam Piping*, Final Report to Electric Power Research Institute on Research Project 1403-13, Combustion Engineering, Chattanooga, Tenn.

Ferro, P. D., Black, R. D., and Li, C-Y. 1990. "Metallurgical Effects on the Flow Properties of Modified Austenitic Alloys," pp. 261-72 in *Proceedings of the Fourth Annual Conference on Fossil Energy Materials*, ORNL/FMP-90/1, Martin Marietta Energy Systems, Inc., Oak Ridge Natl. Lab.

Flately, T., Latham, E. P., and Morris, C. W. 1987. "CEGB Experience with Co-Extruded Tubes for Superheated and Evaporative Sections of PF Fired Boilers," pp. 219-29 in *Advances in Material Technology for Fossil Power Plants*, American Society for Metals International, Materials Park, Ohio.

Goodwin, G. M. 1987. "Development of a New Hot-Cracking Test—The Sigmajig," *Weld. J. (Miami)*, **66**, 33s-38s.

Harries, D. R. 1982. "Physical Metallurgy of Fe-Cr-Ni Austenitic Steels," pp. 1-14 in *Mechanical Behavior and Nuclear Applications of Stainless Steel at Elevated Temperatures*, The Metals Society, London.

Haynes 1989. *Alloy HR-120 for Industrial Heating Applications*, Haynes International, Kokomo, Ind.

INCO 1986. *Incoloy alloys 800 and 800HT*, Inco Alloys International, Inc., Huntington, W.Va.

Irvine, K. J., Gladman, T., and Pickering, F. B. 1969. "The Strength of Austenitic Stainless Steels," *J. Iron Steel Inst.*, **207**, 1017-28.

Kanazawa, K., Yamaguchi, K., and Nishijima, S. 1988. "Mapping of Low Cycle Fatigue Mechanisms at Elevated Temperatures for an Austenitic Stainless Steel," pp. 519-30 in *Low Cycle Fatigue*, ASTM STP 942, American Society for Testing and Materials, Philadelphia.

Keown, S. R., and Pickering, F. B. 1972. "Effect of Niobium Carbide on the Creep Rupture Properties of Austenitic Stainless Steels," pp. 134-43 in *Creep Strength in Steel and High-Temperature Alloys*, The Metals Society, London.

LeBeau, S. E. 1990. Evaluation of the Fabricability of Advanced Austenitic Tubing, *Fossil Energy Advanced Research and Technology Development Materials Program Semiannual Progress Report for Period Ending September 30, 1989*, ORNL/FMP-89/2, Martin Marietta Energy Systems, Inc., Oak Ridge Natl. Lab., pp. 219-27.

Lister, E., Mickleraith, J., and Higgenbottom, A. "High Temperature Properties of Steampipe Welds," pp. 474-81 in *High Temperature Properties of Steels*, Publication 97, Iron and Steel Institute, London.

Lundin, C. D., et al. 1985. "New Concepts in Varestraint Testing for Hot Cracking," *Welding Research the State of the Art, Proceedings of the JDC University Symposium*, 1985 International Welding Congress, American Society for Metals, Toronto.

Lundin, C. D., Qiao, C. Y. P., Gill, T. P. S., and Ren, W. 1989. *The Hot Ductility and Hot Cracking Behavior of Modified 316 Stainless Steels Designed for High Temperature Service*, ORNL/Sub/88-07685/01, Martin Marietta Energy Systems, Inc., Oak Ridge Natl. Lab.

Manjoine, M. J. 1975. "Ductility Indices at Elevated Temperatures," *J. Eng. Mater. Technol.*, **97**, 156-60.

Marshall, P. 1984. *Austenitic Stainless Steels Microstructure and Properties*, Elsevier Science Publishing Co., Inc., New York.

Maziasz, P. J. 1988. "Microstructural Stability for Improved Irradiation Resistance and for High Temperature Strength of Austenitic Stainless Steels," pp. 116-65 in *MiCon 86: Optimization of Processing, Properties, and Service Performance Through Microstructural Control*, ASTM STP 979, American Society for Testing and Materials, Philadephia.

Maziasz, P. J. 1989. "Developing an Austenitic Stainless Steel for Improved Performance in Fossil Power Facilities," *J. Met.* **41**, 14-20.

Maziasz, P. J., and McHargue, C. J. 1987. "Microstructural Evolution in Annealed Austenitic Steels during Neutron Irradiation," *Int. Metall. Rev.* **32**, 190-218.

McCoy, H. E., and King, J. F. 1985. *Evaluation of HD 556 and Incoloy 802 for High-Temparature Gas-Cooled Reactor Applications*, ORNL/TM-9382, Martin Marietta Energy Systems, Inc., Oak Ridge Natl. Lab.

Menard, P. W. K. 1952. *Sigma Phase in Austenitic Stainless Steels*, Final Report P-12-121, United States Steel Company, Irvine Works, Irvine, Calif.

Myllykosi, L. 1983. "Hot Ductility of Austenitic Stainless Steels," pp. 61-66 in *Third Scandinavian Sumposium in Materials Science.*

Nakabayashi, Y. et al. 1986. *Field Test and Evaluation of High Temperature Materials for Ultra Super Critical (USC) Power Boiler*, Technical Review, Mitsubishi Heavy Industries, Ltd., Tokyo.

Nilsson, J-O 1988. "Effect of Nitrogen on Creep-Fatigue Interaction in Austenitic Stainless Steels at 600°C," ASTM STP 942, pp. 543-57 in *Low Cycle Fatigue,* American Society for Testing and Materials, Philadelphia.

Payson, P., and Savage, C. H. 1947. "Changes in Austenitic Chromium-Nickel Steels During Exposure at 1100°F to 1700°F," *Trans. Am. Soc. Met.* **39**, 404-39.

Pickering, F. B. 1979. "Introduction," pp. 1-49 in *The Metallurgical Evolution on Stainless Steels*, American Society for Metals, Materials Park, Ohio.

Plumley, A. L., and Rozniak, W. R. 1989. "Coal Ash Corrosion Field Testing of Advanced Boiler Tube Materials - II," paper 34-1, *Second International Conference on Improved Coal Fired Power Plants*, EPRI publication GS-6422, Electric Power Research Institute, Palo Alto, Calif.

Rehn, I. M. 1981. *Corrosion Problems in Coal Fired Boiler Superheater and Reheater Tubes: Steam Side Oxidation and Exfoliation*, EPRI CS-1812, Electric Power Research Institute, Palo Alto, Calif.

Rittenhouse, P. L. et al. 1985. *Assessment of Materials Needs for Advanced Steam Cycle Coal Fired Plants*, ORNL-6274, Martin Marietta Energy Systems, Inc., Oak Ridge Natl. Lab.

Roberts, D. I., Ryder, R. H., and Viswanathan, R. 1985. "Performance of Dissimilar Welds in Service, 1985," pp. 55-63 in *Residual-Life Assessment, Nondestructive Examination, and Nuclear Heat Exchanger Materials*, PVP-Vol. 98-1, American Society of Mechanical Engineers, New York.

Robinson, E. L. 1952. "Effect of Temperature Variation on Long Time Rupture Strength of Steels," *Trans. ASME* **74**, 777-81.

Sawaragi, Y., Teranishi, H., and Yoshikawa, K. 1988. "The Developement of Newly Steel with High Elevated Temperature Strength and High Corrosion Resistance for Boiler," pp. 238-44 in *Proceedings, International Conference on Creep*, Japan Society of Mechanical Engineers, Tokyo.

Smith, A. B. 1978. "The Effect of Tensile and Compressive Cold Straining on the Properties of Ni-Fe-Cr Alloy," pp. 159-68 in *Characterization of Materials for Service at Elevated Temperatures*, MPC-7, American Society of Mechanical Engineers, New York.

Smith, G. D. and Lipscomb, W. G. 1987. "Corrosion Resistance of a New Composite Tubing Designed for Fluidized Bed Coal Combustions," *Advances in Material Technology for Fossil Power Plants*, American Society for Metals International, Materials Park, Ohio.

Smith, G. 1991. INCO Alloys International, private communication to R. W. Swindeman, Martin Marietta Energy Systems, Inc., Oak Ridge Natl. Lab., February 12.

Swindeman, R. W. et al. 1986. *Alloy Design Criteria and Evaluation Methods for Advanced Austenitic Alloys in Steam Service*, ORNL-6274, Martin Marietta Energy Systems, Inc., Oak Ridge Natl. Lab..

Takahashi, T., et al. 1989. "Development of a High Strength 25Ni-20Cr Steel for Tubes in Ultra Supercritical Power Boilers," paper 41-1, *Second International Conference on Improved Coal Fired Power Plants*, EPRI publication GS-6422, Electric Power Research Institute, Palo Alto, Calif.

Tavassoli, A. A., and Colombe, G. 1978. "Mechanical and Microstructural Properties of Alloy 800," *Metall. Trans.* **9A**, 1203-11.

Topolski, M. 1991. *Evaluation of the Fabricability of Advanced Austenitic Tubing,* Final Report CRD #1207, RDD:91:4500-01-01:01, Babcock & Wilcox Alliance Research Center, Alliance, Ohio.

Trestor, P. W., Johnson, W. R., Simnad, M. T., Burnette, R. D., and Roberts, D. I. 1982. *Assessment of Effects of Ft. St. Vrain HTGR Primary Coolant on Alloy 800,* Report NP-2548, Electric Power Research Institute, Palo Alto, Calif.

Van Weele, S., and Blough, J. L. 1990. *Literature Search Update Fireside Corrosion Testing of Candidate Superheater Tube Alloys, Coatings, and Claddings,* Topical Report Project No. 9-61-5329, Foster Wheeler Development Corporation, Livingston, N.J.

Villagrana, R. E., Kaae, J. L., Ellis, J. R., and Gantzel, P. K. 1978. "The Effect of Aging and Cold Working on the High Temperature Low Cycle Fatigue Behavior of Alloy 800H: Part 1. The Effect of Hardening Processes on the Initial Stress-Strain Curve," *Metall. Trans.* **9A**, 927-34.

Viswanathan, R. 1989. American Society for Metals International, Materials Park, Ohio.

Wolowodiuk, W., Blough, J. L., and Kihara, S. 1989. "Coal-Ash Corrosion--An Update," paper 32-1, *Second International Conference on Improved Coal Fired Power Plants,* EPRI publication CS-6422, Electric Power Research Institute, Palo Alto, Calif.

Yoshikawa, K., Sawaragi, Y., and Yuzawa, H. 1988, 1989. "Development of New Boiler Tubes with High Elevated Temperature Strength and High Corrosion Resistance," paper 5-167, *First International Conference on Improved Coal Fired Power Plants,* EPRI publication CS-5581-SR, Electric Power Research Institute, Palo Alto, Calif.

Yukawa, S. 1991. Private communication to R. W. Swindeman.

INTERNAL DISTRIBUTION

1-2. Central Research Library
3. Document Reference Section
4-5. Laboratory Records Department
6. Laboratory Records, ORNL RC
7. ORNL Patent
8-10. M&C Records Office
11. D. J. Alexander
12. P. Angelini
13. G. C. Bell
14. C. R. Brinkman
15. P. T. Carlson
16. N. C. Cole
17. J. H. DeVan
18. J. R. DiStefano
19. G. M. Goodwin
20. M. L. Grossbeck
21. F. M. Haggag
22. D. O. Hobson
23. R. S. Holcomb
24. L. L. Horton
25. R. R. Judkins
26. J. R. Keiser
27. O. F. Kimball
28. J. F. King
29-33. P. J. Maziasz
34. H. E. McCoy
35. P. L. Rittenhouse
36. G. M. Slaughter
37. J. O. Stiegler
38. R. Strehlow
39-43. R. W. Swindeman
44. V. J. Tennery
45. P. F. Tortorelli
46. J. R. Weir
47. D. F. Wilson
48. A. D. Brailsford (Consultant)
49. Y. A. Chang (Consultant)
50. H. W. Foglesong (Consultant)
51. J. J. Hren (Consultant)
52. M. L. Savitz (Consultant)
53. J. B. Wachtman, Jr. (Consultant)

EXTERNAL DISTRIBUTION

54-55. ARGONNE NATIONAL LABORATORY, 9700 S. Cass Avenue, Argonne, IL 600439

W. A. Ellingson
K. Natesan

56. BABCOCK & WILCOX, Fossil River Power Generation Division,, 20 South Van Buren Avenue, Barberton, OHG 44203

W. C. Mack

57. BABCOCK & WILCOX RESEARCH LABORATORY, 1562 Beeson Street, Alliance, OH 44601

M. J. Toploski

58. CABOT CORPORATION, Corrosion Resistant Alloys, 1020 West Park Avenue, Kokomo, IN 46901

A. I. Asphahani

59. CARPENTER TECHNOLOGY CORP., Steel Division, P.O. Box 62, Reading, PA 29603

J. W. Martin

60. CHICAGO BRIDGE AND IRON COMPANY, 800 Jorie Blvd., Oak Brook, IL 60521

E. Uptis

61. ROBERT L. CLOUD AND ASSOCIATES, 125 University Ave., Berkeley, CA 94710

W. R. Milesell

62-63. COMBUSTION ENGINEERING, INC., 911 W. Main Street, Chattanooga, TN 37402

D. A. Canonico
B. Roberts

64. COMMISION OF THE EUROPEAN COMMUNITIES, Petten Establishment, Postbus 2, 1755 ZG Petten, The Netherlands

Marcel Van de Voorde

65. CORNELL UNIVERSITY, Materials Sciences and Engineering Department, Bard Hall, Ithaca, NY 14853

Che-Yu Li

66-69. ELECTRIC POWER RESEARCH INSTITUTE, 3412 Hillview Avenue, P.O. Box 10412, Palo Alto, CA 94303

W. T. Bakker
R. I. Jaffee
J. Stringer
R. Viswanathan

70. EXXON RESEARCH AND ENGINEERING CO., P.O. Box 101, Florham Park, NJ 07932

M. J. Humphries

71. FOSTER WHEELER DEVELOPMENT CORPORATION, 12 Peach Tree Hill Road, Livingston, NJ 07039

J. Blough

72. GA TECHNOLOGIES, INC., Reactor Structural Materials Branch, Fuels and Materials Division, P.O. Box 81608, San Diego, CA 92138

D. I. Roberts

73. GENERAL ELECTRIC COMPANY, Turbine Materials Engineering, Building 41, Room 306, 1 Riber Road, Schenectady, NY 12345

    J. Pepe

74. GILBERT ASSOCIATES, INC., Morgantown Road, Green Hills, Reading, PA 19603

    R. L. Dail

75. INCO ALLOYS INTERNATIONAL, INC., P.O. 1958, Huntington, WV 25720

    T. H. Bassford

76. LUKENS STEEL COMPANY, R&D Center, Coatesville, PA 19320

    J. Gulya

77. THE MATERIALS PROPERTIES COUNCIL, INC., United Engineering Center, 345 E. 47th Street, New York, NY 10017

    M. Prager

78. NATIONAL MATERIALS ADVISORY BOARD, National Research Council, 2101 Constitution Avenue, Washington, DC 20418

    Z. M. Zwilsky

79. OFFICE OF NAVAL RESEARCH, Code 431, 800 N. Quincy Street, Arlington, VA 22217

    S. G. Fishman

80. STANDARD OIL, INDIANA, P.O. Box 400 - MS B-8, Naperville, IL 60540

    S. Ibarra

81. STONE AND WEBSTER ENGINEERING CORPORATION, 245 Summer Street, P.O. Box 2325, Boston, MA 02107

    M. P. Berardi

82. SUPERIOR TUBE COMPANY, P. O. Box 191, Norristown, PA 19404

    C. C. Matthews

83. TENNESSEE VALLEY AUTHORITY, Metallurgical & NDT Section, 820 Chestnut Street, Tower II, Chattanooga, TN 37401

    S. O. Hilton

84. R. D. THOMAS AND COMPANY, INC., 103 Avon Road, Narberth, PA 19072

R. D. Thomas, Jr.

85-86. UNIVERSITY OF CALIFORNIA AT BERKELEY, Department of Materials Science and Mineral Engineering, Berkeley, CA 94720

E. R. Parker
R. O. Ritchie

87. UNIVERSITY OF ILLINOIS,. Department of Mechanical and Industrial Engineering, 1206 W. Green Street, Urbana, IL 61801

D. L. Marriott

88. UNIVERSITY OF MANCHESTER INSTITUTE OF SCIENCE AND TECHNOLOGY, P.O. Box 88, Manchester, M601QD, United Kingdom

F. J. Stout

89. UNIVERSITY OF PITTSBURGH, Department of Metallurgical and Materials Engineering, 848 Benedum Hall, Pittsburgh, PA 15261

G. H. Meier

90. UNIVERSITY OF TENNESSEE, Department of Materials Science, Knoxville, TN 37996

C. D. Lundin

91. DOE, ENERGY CONVERSION AND UTILIZATION TECHNOLOGIES DIVISION, CE-14, 5E-091 Forrestal Building, Washington, DC 20585

J. J. Eberhardt

92-93. DOE Field Office, P.O. BOX 2001, Oak Ridge, TN 37831

Office of Deputy Assistant Manager for Energy Research and Development
E. E. Hoffman

94. DOE, OFFICE OF BASIC ENERGY SCIENCES, Materials Sciences Division, ER-131, J314/GTN, Washington, DC 20585

F. V. Nolfi, Jr.

95-96. DOE, OFFICE OF FOSSIL ENERGY, Washington, DC 20585

J. P. Carr (FE-24, C179/GTN)
R. E. Harrington (FE-20, C164/GTN)

97. DOE, OFFICE OF VEHICLE AND ENGINE R&D , CE-131, 5G-064 Forrestal Building, Washington, DC 20585

R. B. Schultz

98-102. DOE, MORGANTOWN ENERGY TECHNOLOGY CENTER, P.O. Box 880, Morgantown, WV 26505

J. W. Byam, Jr.
D. Dubis
V. P. Kothari
J. E. Sholes
J. S. Wilson

103-106. DOE, PITTSBURGH ENERGY TECHNOLOGY CENTER, P.O. Box 10940, Pittsburgh, PA 15236

R. A. Carabetta
S. W. Chun
J. J. Joubert
F. W. Steffgen

107-116. DOE, OFFICE OF SCIENTIFIC AND TECHNICAL INFORMATION, P.O. Box 62, Oak Ridge, TN 37831

For distribution by microfiche as shown in DOE/OSTI-4500, Distribution Categories UC-103 (Fluidized Bed Combustion) and UC-114 (Coal-Based Materials and Components)